AD-A070 175 TEXAS UNIV AT AUSTIN ELECTRICAL GEOPHYSICS RESEARCH LAB F/G 8/7
MAGNETOTELLURIC AND DC DIPOLE-DIPOLE SOUNDINGS IN NORTHERN WISC--ETC(U)
MAY 77 F X BOSTICK, H W SMITH, J E BOEHL N00014-76-C-0484

UNCLASSIFIED NL

| OF |
AD
A070175

END
DATE
FILMED
7-79
DDC

MAGNETOTELLURIC AND DC DIPOLE-DIPOLE SOUNDINGS IN NORTHERN WISCONSIN

By

F. X. Bostick, Jr., H. W. Smith, and J. E. Boehl

Final Technical Report

May 15, 1977

ELECTRICAL GEOPHYSICS RESEARCH LABORATORY

prepared under

Contract N00014-76-C-0484

Office of Naval Research, Washington, DC

and

GRANT GA 38827

National Science Foundation

ELECTRICAL ENGINEERING RESEARCH LABORATORY
THE UNIVERSITY OF TEXAS AT AUSTIN

MAGNETOTELLURIC AND DC DIPOLE-DIPOLE SOUNDINGS IN NORTHERN WISCONSIN

By

F.X. Bostick, Jr., H.W. Smith, and J.E. Boehl

Final Technical Report
May 15, 1977

S/C ELECTRICAL GEOPHYSICS RESEARCH LABORATORY

prepared under

Contract N00014-76-C-0484, NSF-GA-38827

Office of Naval Research, Washington, DC

and

GRANT GA 38827

National Science Foundation

ELECTRICAL ENGINEERING RESEARCH LABORATORY

THE UNIVERSITY OF TEXAS AT AUSTIN

ABSTRACT

During the summer of 1974 this Laboratory participated in a joint study of the crust in northern Wisconsin with the Colorado School of Mines, the University of Wisconsin at Madison and others. The Wisconsin Arch region was selected for the large areal extent of outcrop of highly resistive crystalline basement rocks considered most favorable for possible lithospheric propagation of low frequency electromagnetic waves. The principal objective of the joint study was the determination of the maximum resistivity and thickness of a highly resistant zone underlying a thin surface layer of glacial till over most of the area. It was recognized at the outset that a combination of deep DC resistivity sounding, which can determine the resistivity-thickness product of the resistant zone, and the magnetotelluric method, which can determine its thickness, would be required. DC dipole-dipole measurements made at 21 sites in the area encountered a highly conductive feature to the southeast of the fixed source dipole antennas in the direction of the maximum lateral extent of the outcrop. This feature, which is referred to as the Flambeau Anomaly, attenuated the transmissions from the dipole antennas and thus distorted the resistivity-thickness product results obtained by this Laboratory. However, magnetotelluric soundings provided estimates for the thickness of the resistant zone in the region southeast of the anomaly where DC dipole-dipole results by the Colorado School of Mines group indicate very high values for the resistivity-thickness products. By combining these results

it is possible to estimate the resistivity of the resistant zone and its thickness. Results of this survey are presented along with some innovative methods for the analysis and inversion of magnetotelluric data.

TABLE OF CONTENTS

LIST OF FIGURES

INTRODUCTION

During the summer of 1974, the Electrical Geoscience Laboratory of The University of Texas at Austin (UTA) made a number of geoelectric measurements over the area of exposed crystalline basement rocks of the Wisconsin Arch. The measurements were part of a joint study of the crust of the region made by groups from the Colorado School of Mines (CSM), Keller and Furgerson, (1977), the University of Wisconsin at Madison (UWM), Sternberg and Clay, (1977), and The University of Texas at Dallas (UTD). In addition to the general scientific objectives of the study specific interest was directed to the measurement of the electrical resistivity versus depth in the upper crust in order to evaluate the feasibility of using the lithosphere as a path for electromagnetic communications. Critical to the successful operation of a long range high data rate lithospheric communications system would be the existence of resistivities in excess of 10^6 Ω - M. Measurements from the surface of resistivities of this order in the crustal rocks at depth provided a challenge to the design of the experiment.

In most areas of the continental United States a conductive overburden obscures the true maximum resistivity values of the substrata from surface measurement. However, the relatively thin and resistive cover of glacial till overlying the outcrop of basement rocks in northern Wisconsin offers a favorable setting for the measurement of large resistivity values at depth. This was a major consideration in the selection of northern Wisconsin as a site for the experiment.

The choice of survey methods was based on a simple model of the average characteristics of the crustal resistivities of the region. The elements of the model were suggested by the results of previous studies, Davidson et al., (1974), Dowling, (1970). A superficial cover of glacial till varies in thickness from 10 to 100 meters. Near surface resistivities range from one hundred to several hundred ohm meters. Beneath this cover the bulk resistivity increases rapidly with depth as the pressure closes the water filled voids in the insulating solid matrix of the basement rocks. The resistivity increase continues to a maximum. Both the depth to the maximum and the resistivity at that depth were unknown; however, estimates placed the depth at between 5 km and 10 km. Below the maximum, the resistivity begins a slow monotonic decrease with depth as ionic conduction, stimulated by the increasing temperature, enhances the conductivity of the rocks. In summary, the average resistivity versus depth curve shows a single mode, increasing monotonically from a minimum at the surfact through a maximum into a uniform decrease. Each of the survey techniques considered was tested by evaluating its response to a horizontally uniform earth having this distribution of resistivity with depth.

Even for this relatively simple test model, no one sounding technique proved to be capable of resolving all of the significant parameters. A survey involving a combination of methods with complementary response characteristics was considered essential. The UTA group chose to combine DC dipole-dipole measurements with a magnetotelluric (MT) survey to achieve the desired objectives.

The DC dipole-dipole method of resistivity sounding involves the measurement of signals transmitted by a dipole antenna, Keller, (1966). The measurements are made with a dipole receiving antenna and are obtained as a function of separation between the transmitter and receiver. The measured signal levels are usually converted to apparent resistivities and plotted versus separation. The apparent resistivity at a site is defined as the resistivity value for a homogeneous half space that would produce the same signal at the site from the dipole transmitter as was actually measured. Over a horizontally uniform earth the depth of penetration of the measurement increases monotonically with transmitter receiver separation. The shape of the apparent resistivity versus separation curve corresponds in a general way to the shape of the resistivity versus depth in the section. For this reason, the apparent resistivity curves are often used directly as a rough indication of resistivity versus depth. A section interpreted in this way is called a psuedo section.

For the single mode resistivity versus depth curve described above, the apparent resistivity versus separation curve also has a single mode. The separation at which the maximum occurs and the apparent resistivity at the maximum depend principally upon two parameters. One is the surface conductance, S, where

$$S(z_1) = \int_0^{z_1} \sigma(z)\, dz, \qquad (1)$$

σ is the conductivity derived as the reciprocal of the resistivity, ρ, and z is depth. The conductance, $S(z)$, increases monotonically with depth,

rapidly at first, to become almost constant as ρ decreases from a maximum near the surface. The upper limit, z_1, of the conductance integral is any value of z large enough to yield this almost constant value for $S(z)$. For the conductivity functions expected to be typical of the shield area of northern Wisconsin z_1 should be considerably less than the depth to the mode, z_m.

The second parameter affecting the mode of the apparent resistivity curve is the transverse resistance, T, where

$$T = \int_{z_2}^{z_3} \rho \, dz \tag{2}$$

and $z_2 < z_m < z_3$. Most of the value of the integral comes from the neighborhood of the mode. The limits of the integral extend either side of the mode to points outside which the decreasing resistivity values are so small that they make no significant contribution to the integral.

The exact value of separation at which the mode of the apparent resistivity occurs depends upon the bearing to the receiver site relative to the transmitting dipole axis. However, this separation is roughly given by the simple expression

$$r_m \approx \sqrt{ST} . \tag{3}$$

The apparent resitivity, ρ_{AM}, at the mode is expressed approximately by

$$\rho_{AM} \approx \frac{\sqrt{T}}{S} . \tag{4}$$

These two relations are strictly applicable only to the case of a horizontally uniform earth. It was anticipated that lateral resistivity variations would most certainly occur in the Wisconsin survey. However, it was hoped

that these variations would be confined to the surface and would represent local deviations from a regional average. If such were the case, scatter would indeed be imparted to the measured apparent resistivities, but smoothing techniques could be used to extract the average trends of the curve. In particular, it was hoped that the significant features of the mode could be identified. If so, the parameters S and T could be estimated from the DC dipole-dipole measurements. These estimates would be combined with the MT results to provide an indication of the subsurface resistivities.

A priori estimates of the values of S and T that would be encountered were used to design the coverage of the DC dipole-dipole measurements. It was felt that a value of S as large as 1 mho could exist. In addition, the survey should be capable of measuring values of T ranging up to 10^{11} ohm-square meters. Substituting these values into (3) shows that separations as large as 300 km would be required to identify the mode.

A separation of 300 km between the transmitter and receiver could result in very small signal strengths at the receiver. For this reason, it was decided to use the large 22 km long crossed dipole antennas at the U.S. Navy's Wisconsin Test Facility (WTF) located near Clam Lake, Wisconsin. This had the advantage of providing a large dipole moment for the transmitter and would increase the signal levels at the receiver. It would have the disadvantage of fixing the location of the transmitter. This disadvantage later proved to be costly in terms of applying the dipole-dipole measurements to the original objectives of the experiment.

Measurements were planned along four raidal traverses extending

from the center of the WTF antennas. As may be seen in Figure 1, the WTF is near the northwest boundary of the basement outcrop. One of the traverses would extend in a southeasterly direction toward the geometric center of the outcrop. It was felt that this traverse offered the best chance for measuring a large value of the parameter T. A separation of 300 km could be obtained without approaching the edge of the outcrop where the presence of conductive sediments would influence the measurements. A second traverse would run slightly north of east with a third extending essentially due south. This would provide fan coverage of the region extending from the antennas toward the side of the outcrop opposite the WTF. One final radial would be run northwesterly across the boundary of the outcrop to define the lateral conductivity transition nearest the antenna. A total of 21 sites were to be occupied with most of them distributed along the four radial traverses. These same sites would also be used for the MT survey.

Using natural electromegnetic background noises as a source of energy MT is capable of sounding deep into the earth's crust. The sounding principle is based upon the fact that the depth of penetration of an electromagnetic wave propagating vertically downward into a horizontally uniform earth bears a reciprocal relationship to the frequency of the wave. The exact nature of the relationship depends upon the distribution of resistivity with depth. A measure of the subsurface resistivity may be derived at any one frequency from the wave impedance computed as the ratio of the intensity of the horizontal electric (E) field to the horizontal magnetic (H) field at the surface. More specifically, the resistivity measure is defined as that value of

resistivity for a homogeneous half space that would produce the same magnitude of the wave impedance as derived from the experimental data. This measure is called the apparent resistivity. A frequency plot of the apparent resistivy computed from Fourier analyzed E and H field time series data can be used as an indication of the resistivity versus depth beneath the measurement site. It should be remembered that depth is reciprocally related to frequency.

The sensitivity of the MT method was tested by computing the apparent resistivity vs frequency curve for a horizontally uniform earth having resistivity versus depth equal to the single mode test function described above. The resulting apparent resistivity curve also has a single mode. The principal diagnostic features of this computed curve are the skirts of the mode. The skirt on the high frequency side of the maximum tends to follow an asymptote determined by the value of the surface conductance, S, defined above, Berdechevsky, (1968). The depth, D, to the significant thermally induced conductivity increase below the mode determines the asymptote of the low frequency skirt. The measure of S is redundant with the dipole-dipole results but the indicated value of D is complementary. It is complementary in the sense that it can be used with the value of T derived from the dipole-dipole measurements to produce an estimate of the subsurface resistivity. This is demonstrated as follows: using D for z_3 the upper limit of the integral in (2), one obtains

$$T = \int_{z_2}^{D} \rho dz \qquad (5)$$

If ρ is small for $z < z_a$ compared to its value in the neighborhood of the mode, then

$$T \approx \int_0^D \rho dz \tag{6}$$

The resistivity ρ_{ave} is defined as

$$\rho_{ave} \triangleq \frac{1}{D} \int_0^D \rho dz \tag{7}$$

Since ρ is positive for all z it follows that

$$\rho_{max} > \rho_{ave} \tag{8}$$

where ρ_{max} is the largest value of ρ in the interval $o < z < D$. The resistivity ρ_{ave} can, therefore, be used as an estimate of the lower bound for ρ. Substituting from (6) and (7) into (8) one obtains

$$\rho_{max} > \frac{T}{D}$$

where T is found from the dipole-dipole measurements and D is derived from the MT data.

DC DIPOLE-DIPOLE RESULTS

Most of the twenty-one DC dipole-dipole sites in Figure 1 lie along four roughly radial lines from the WTF antennas. The Namekagon (Na), Lake Owen (O) and Northwest Chequamegon (NC) sites form the northwest radial; Flambeau (F), South Flambeau (SF), and South Chequamegon (SC) form the south radial; Spillerberg Lake (Sp), Morse(M), Island Lake (I), Chaney Lake (C), Gogebic (G), and Sidnaw (Si) comprise the northeast radial; and the Bear Lake (B), Flambeau (F), Sailor Lake (Sa), Guadalcanal (Gu), Tomahawk (T), and Elton (E) sites make up the longest radial to the southeast. The

apparent resistivities calculated for each site represent the maximum value produced by a synthetic vector rotation of the source dipole, Keller and Ferguson, (1977). A plot of these apparent resistivities vs separation distance from the center of the WTF antennas is shown in Figure 2. Lines are drawn connecting the points to indicate three of the radials. Values along the south radial were similar to the southeast radial and are not shown to avoid undue complication of the Figure.

The highest apparent resistivities were measured along the northeast radial in Figure 2 except for the Sidnaw (Si) site which shows a sharp drop in resistivity. It is possible that this decrease is due to a conductivity anomaly in the vicinity of that site since it lies within the outcrop area shown in Figure 1 where uniformly high resistivities were anticipated.

Measurements along the northwest radial were terminated after low apparent resistivity was encountered at the Northwest Chequamegon (NC) site. This result was expected since that site lies beyond the outcrop in Figure 1 where a thickening of the conductive sedimentary overburden occurs.

The southeast radial in Figure 2 was expected to produce the highest measured apparent resistivities. This hypothesis was based on the fact that this direction is toward the center of the outcrop area and severe lateral changes in resistivity were not anticipated. However, a precipitous drop in the apparent resistivity is seen to occur at the Flambeau (F) site which is caused by the presence of a large highly conductive feature encountered by both the UMW and UTA groups and referred to as the Flambeau Anomaly.

This feature is evident in the DC dipole-dipole and MT results at a number of sites and has been studied in detail by the UMW group, Sternberg and Clay, (1977). The approximate extent of the anomaly is indicated in Figure 1. Beyond the Flambeau (F) site, the apparent resistivity in Figure 2 climbs steadily at the successive sites along this radial; Sailor Lake (Sa), Guadalcanal (Gu), Tomahawk (T), and finally Elton (E) at a distance of 185 km from the WTF antennas. However, it is apparent that the measured resistivities at these sites beyond the Flambeau Anomaly are greatly depressed by its presence. It is also significant that the very low apparent resistivities at the Flambeau (F) site were measured from both WTF antennas. This fact, plus the slow steady rise in resistivity with separation distance beyond the anomaly suggests that the conductive feature extends to considerable depth as well as lateral extent. Sternberg and Clay, (1977) reach the same conclusion.

One additional measurement also has significance relative to the above observations. By chance, during the recording of relatively weak signals from the WTF antennas at our Guadalcanal (Gu) site on the southeast radial, we happened to receive clearly distinctive signals from the CSM source dipole some 70 km away to the southwest. These CSM signals were, at least, an order of magnitude greater than those from the WTF antennas. When adjustments are made for the difference in dipole source moments and distances the apparent resistivity value calculated from the CSM dipole was approximately 10^5 ohm-meters, the highest value observed at any of our sites. The apparent resistivity measured at this same site from the WTF antennas was

approximately 500 ohm-meters. We attribute most of the factor of 200 difference in the two measured apparent resistivities to the signal attenuation of the Flambeau Anomaly which lies across the transmission path from the WTF antennas. In contrast, the path from the CSM dipole lies well to the south of the anomaly. Our measurement from the CSM dipole at this site is consistent with the high resistivitiy values observed by that group in the same general area.

MAGNETOTELLURIC PRINCIPLES

The Magnetotelluric (MT) method has been described by Cagniard (1953), Cantwell and Madden (1960), Wait (1962), Swift (1969), Vozoff (1972) and many others. For a layered earth, an apparent resistivity is computed from the ratio of the horizontal electric field (E) to the orthogonal horizontal magnetic field (H)

$$\rho_a = \frac{0.2}{f} \left|\frac{E}{H}\right|^2 \tag{9}$$

where f is frequency. While adequate for a layered earth, Equation (9) may give distorted results in regions where the earth has a more complicated structure. An impedance tensor model, Cantwell (1960), Bostick and Smith (1962), and Swift (1967), is required for two dimensional structures. Here the tensor relations between the E and H field may be expressed as

$$[E] = [Z]\,[H] \tag{10}$$

or

$$E_x = Z_{xx} H_x + Z_{xy} H_y \tag{11}$$

$$E_y = Z_{yx} H_x + Z_{yy} H_y$$

where the tensor impedance is

$$[Z] = \begin{bmatrix} Z_{xx} & Z_{xy} \\ Z_{yx} & Z_{yy} \end{bmatrix} \tag{12}$$

For two dimensional structures the principal impedance values Z'_{xy} and Z'_{yx} are calculated with axes parallel and perpendicular to the strike of the two dimensional inhomogeneity. If the data appear to indicate three dimensional qualities, the same model is used in an attempt to extract from the results a two dimensional fit. The principal impedance tensor, [Z'], is related to the original one, [Z], by the following equation:

$$[Z'] = [T]\,[Z]\,[T]^{-1} \tag{13}$$

where

$$[T] = \begin{bmatrix} \cos\theta & \sin\theta \\ -\sin\theta & \cos\theta \end{bmatrix} \tag{14}$$

Moreover, the principal impedance tensor is related to the measured E and H fields as follows:

$$[T]\,[E] = [Z']\,[T]\,[H] \tag{15}$$

In this paper, Equation (15) rather than Equation (13) is used to calculate the principal impedance tensor, that is, instead of rotating the impedance tensor to the principal axes, Sims and Bostick (1969), Hermance (1973), the E and H fields are rotated to the principal axes and then the tensor estimates are computed. The rotation angle, φ, which maximizes $|Z_{xy}|^2 + |Z_{yx}|^2$ is given by Swift (1967) as

$$\tan 4\varphi = \frac{(Z_{xx} - Z_{yy})(Z_{xy} + Z_{yx})^* + (Z_{xx} + Z_{yy})^* (Z_{xy} + Z_{yx})}{|Z_{xx} - Z_{yy}|^2 - |Z_{xy} + Z_{yx}|^2} \quad (16)$$

For a strictly two dimensional structure Z'_{xx} and Z'_{yy} are zero, and the tensor decouples into two modes represented by:

$$\begin{aligned} E'_x &= Z'_{xy} H'_y \\ E'_y &= -Z'_{yx} H'_x \end{aligned} \quad (17)$$

where

$$[E'] = [T][E] \quad (18)$$

and

$$[H'] = [T][H]$$

From the principal impedance values Z'_{xy} and Z'_{yx}, the principal apparent resistivity values are computed as

$$\begin{aligned} \rho_{xy}' &= \frac{0.2}{f} |Z'_{xy}|^2 \\ \rho_{yx}' &= \frac{0.2}{f} |Z'_{yx}|^2 \end{aligned} \quad (19)$$

Associated with the principal impedances are the respective phases

$$\begin{aligned} \Psi'_{xy} &= \tan^{-1} \frac{I'_{xy}}{R'_{xy}} \\ \Psi'_{yx} &= \tan^{-1} \frac{I'_{yx}}{R'_{yx}} \end{aligned} \quad (20)$$

where the R's and I's are the real and imaginary parts, respectively of the Z's.

Once the two principal axes have been determined there remains the task of identifying which one of the two represents the strike direction.

This is typically done by correlating the vertical component of the magnetic field with a horizontal component as a function of azimuth rotation. The strike direction is identified as the direction of the principal axes most nearly perpendicular to the azimuth showing maximum correlation, Vozoff (1972).

When performing one dimensional inversions of apparent resistivity vs frequency curves to produce resistivity vs depth soundings, it is common practice to use the principal axis curve which represents the case of the electric field parallel (E-parallel) to the strike direction. This choice is based largely on the behavior of the E-parallel and E-perpendicular cases in simple two-dimensional models such as vertical faults and dikes where it is observed that the E-parallel inversion curve is continuous across the boundary for these models and the resistivity values at depth are less affected by shallow features, Swift (1969), Vozoff (1972).

MT MEASUREMENTS AND ANALYSIS

MT and AMT measurements were made in the frequency ranges extending from .03 to 10 Hz and from 10 Hz to 800 Hz, respectively. The methods used for processing the data may be summarized briefly as follows:

(1) The first step in the procedure was to obtain the frequency domain transformation of the electric (E) and magnetic (H) field data. The hardware of the AMT receiver directly provided the necessary frequency decomposition throughout the higher of the two frequency bands. These real and imaginary components of the E and H spectra at selected frequencies were

periodically sampled and digitized. A programmable calculator was then used to compute and store the auto and cross power spectrum estimates needed for subsequent analysis.

The AMT receiver used in Wisconsin was not capable of being tuned to frequencies below 10 Hz. In order to utilize the receiver for Fourier decomposition of the data in lower frequency band, an analog recording was made of the real-time E and H field components. The tape was then replayed into the AMT receiver at a higher speed. The real-time frequencies were thus multiplied up to points within the range of the receiver. The power spectrum estimates were then accumulated as outlined above. Thirteen frequencies were chosen to define the spectra from .03 to 800 Hz. From this point on in the analysis process, both bands of frequencies are handled in the same manner and we will use the term MT data to refer to the entire frequency range.

(2) The auto and cross power spectrum estimates were corrected for all system responses.

(3) The principal impedance estimates were calculated after rotating the spectra to the principal axes, where the rotation angle, φ, is determined from Equation (16). The geometric mean of four stable least squared estimates of the principal impedances, Sims, et al, (1971) was chosen.

(4) The principal resistivities and phases were computed from the corresponding estimates as indicated in Equations (19) and (20).

(5) A phase smoothing operation (Appendix II) was applied to the apparent resistivity estimates.

(6) Finally, the one dimensional resistivity vs depth soundings were obtained by a simplified inversion algorithm, Bostick (1977), also (Appendix I).

Equipment limitations at the time of this survey did not permit the measurement of the vertical magnetic field (Hz) component and, hence, we are unable to determine the strike direction of apparent two dimensionalities which were evident in varying degrees at most sites. Also, we cannot determine which of the apparent resistivity curves in the principal axes represent the E-parallel case so that one dimensional inversions are made for both curves.

MT RESULTS

Since the average spacing between adjacent MT sites is more than 20 km, this investigation can only be regarded as a broad reconnaissance survey of the region. Results at eight of the nineteen MT sites occupied during the survey are considered to be the most significant relative to the main objectives of this study and will be presented in this paper. It will be seen that this choice of sites, shown by circles in Figure 1, suggests a highly resistive subsurface to the northeast and southeast of the WTF

antennas and gives evidence of the presence of the highly conductive Flambeau Anomaly. Some of the sites which are omitted, i.e., Northwest Chequamegon (NC), Lake Owen (O), and Sidnaw (Si) are more conductive than those presented. In the case of the Northwest Chequamegon (NC) and Lake Owen (O), the increased conductivity probably indicates a thickening of the sedimentary overburden outside of the indicated extent of the outcrop area in Figure 1. As previously mentioned, the Sidnaw (Si) site may, however, be situated in a local conductivity anomaly in a more resistive area.

Phase smoothed apparent resistivity vs frequency curves in the principal axes are shown in Figures 3 through 10. Indicated on these figures are lines which represent the asymptotes of constant longitudinal conductance, S, of the surface layer in mhos. In other words, the apparent resistivity curves would asymptote these constant S lines if the surface layer were uniform and had the specific S value shown. As seen from these figures, the extremes of all S values lie between 0.1 and 0.7 mhos. A typical value of S = 0.2 to 0.4 mhos seems to be representative.

The simplified one dimensional inversions of both curves in Figures 3 through 10 produce the resistivity vs depth soundings shown in Figures 11 through 18. There is not a one to one correspondence between individual points on the sets of curves representing apparent resistivity vs frequency and resistivity vs depth. This results from a curve fitting and interpolation routine used in the inversion process.

The depths in Figures 11 through 18 are measured from the surface and the shallowest points shown vary with the value of the measured apparent resistivity as well as the highest frequency at each site. Our upper frequency of 800 Hz limited the MT response to depths below 0.3 to 1 km at most sites and the measurements were completely insensitive to the surface layer of glacial till covering most of the region.

As indicated in the section on DC dipole-dipole results, the Flambeau (F) and Park Falls (P) sites clearly lie within or to the southeast of the Flambeau Anomaly with respect to the WTF antennas. Their resistivity vs depth soundings shown in Figures 9 and 10 drop to low values at shallower depths than any of the rest. From the estimated extent of Flambeau Anomaly, Sternberg and Clay (1977), it is possible that the Flambeau (F) site is a few km to the south of the anomaly and the Park Falls (P) site lies within it. The higher conductivity at the latter site would support this conclusion.

The remaining resistivity vs depth soundings in Figures 13 through 18 indicate resistivities in the range from 10^3 to 10^5 ohm-meters at the shallower depths decreasing to levels between ten and a few hundred ohm-meters at the maximum depths. We interpret these results as evidence of a high resistivity zone extending to the northeast and to the southeast of the WTF antennas. On each resistivity vs depth sounding in Figures 13 through 18 we assign a thickness value, t, to this resistive zone for both the maximum and minimum sounding curves. To obtain these thickness values we use the total depth from the surface to the point on the curves where the arbitrary level of

1000 ohm-meters is reached. We neglect the superficial layer of glacial till estimated to be less than 100 m thick over most of the region.

Table 1 summarizes the estimates for the thickness of the resistive zone. Average maximum and minimum values for the six sites are 42 km and 14 km, respectively.

DISCUSSION

The UTA DC dipole-dipole soundings did not produce the very high apparent resistivities values which were expected, particularly for the large dipole separations along the southeast radial. We attribute these results along that radial to the presence of the Flambeau Anomaly. The lone exception was the high apparent resistivity measured from the CSM source dipole at the Guadalcanal (Gu) site where the transmission path lies to the south of the anomaly. Thus, our DC dipole-dipole soundings do not contriubte significantly to the determination of the maximum resistivities of the resistant zone. They are included, however, because they help define the Flambeau Anomaly and because they also yield resistivity information relative to the area to the north of the anomaly. It is fortunate for objectives of the co-operative experiment, however, that the CSM DC dipole-dipole results well to the south of the Flambeau Anomaly indicate very high values for the transverse resistance, T. Combining their results with our thickness values from the MT measurements they estimate resistivity values of at least several million ohm-meters for the high resistivity zone, Keller and Furgerson (1977).

The MT results are somewhat restricted by the lack of vertical

Table 1

SUMMARY ESTIMATES FOR THE THICKNESS
OF THE HIGH RESISTIVITY ZONE

Site Name	Resistive Layer Thickness t_{max} (km)	Resistive Layer Thickness t_{min} (km)
Elton	40	9
Glidden	40	20
Gogebic	70	30
Guadalcanal	30	8
Stevens Lake	10	5
Tomahawk	60	10
Average	39	14

magnetic field data, the upper frequency limit, and the wide separation between sites. Another problem which is more sever in high resistivity regions is the occurence of nearly parallel maximum and minimum apparent resistivity curves over most or all of the frequency range. Dowling (1970) encountered this same problem at most of his MT sites in the Wisconsin Arch. The Guadalcanal (Gu), Tomahawk (T), Elton (E) and Stevens Lake (St) sites in Figures 5 through 8, respectively, are examples of this phenomenon. This situation is not uncommon in MT surveys and is attributed to lateral changes in resistivity at shallow depths in the immediate vicinity of electrodes (DC effect), Keller (1970).

The probable cause for this effect is the fact that the magnetic field responds to the total flow of current over a volume with dimensions of the order of a skin depth, whereas the electric field can respond to changes in resistivity in the immediate vicinity of the electrodes. If recognized in time the DC effect can usually be corrected or minimized by longer electrode lines or with a multiplicity of closely spaced sites. Unfortunately, the DC effect was not discovered until the survey was completed.

Thus, one or both apparent resistivity curves in Figures 5 through 8 could have been shifted up or down by the DC effect, and without additional information we have no way of knowing which curve might be closer to the true level of apparent resistivity. Since the curves remain essentially parallel throughout the frequency range there is no difference in their frequency behavior except for the separation. Thus, if these DC effects

could be removed we would expect the results to be essentially one dimensional yielding a single resistivity vs depth sounding.

We can argue as others have done, Keller (1970), that since the MT method is more responsive to conductive bodies in the vicinity of the electrodes the minimum curve would be lowered more by a conductive anomaly than the maximum curve would be raised by a resistive anomaly. In other words, there might be a statistical bias in favor of the maximum curve, but for any specific case the uncertainty remains. If averages over the region are truly representative, this argument would favor the average thickness values from the maximum resistivity-depth soundings in Table 2.

The capability of the MT method to investigate large scale crustal structure with special emphasis on the detection of conductive anomalies is well known. We believe that it is also capable of measuring the thickness of high resistivity zones with less ambiguity if some of the problems encountered in the present survey are corrected. This survey represents the first field trial of our AMT system which has subsequently been modified extensively, including the addition of a vertical magnetic field channel. In addition, we now compute all of the MT results, including the simplified inversion while at the site or soon thereafter. Thus, the troublesome DC effects, poor quality data, and a variety of other ills can be recognized in time to take remedial action. A more recent MT survey by our group, Stanley, et al, (1977) incorporates these features to eliminate most of the difficulties encountered in Wisconsin survey.

ACKNOWLEDGEMENTS

This work was supported by the Earth Physics Program, Code 463, Office of Naval Research under Contract N00014-76-C-0484 and by the National Science Foundation under Grant GA 38827.

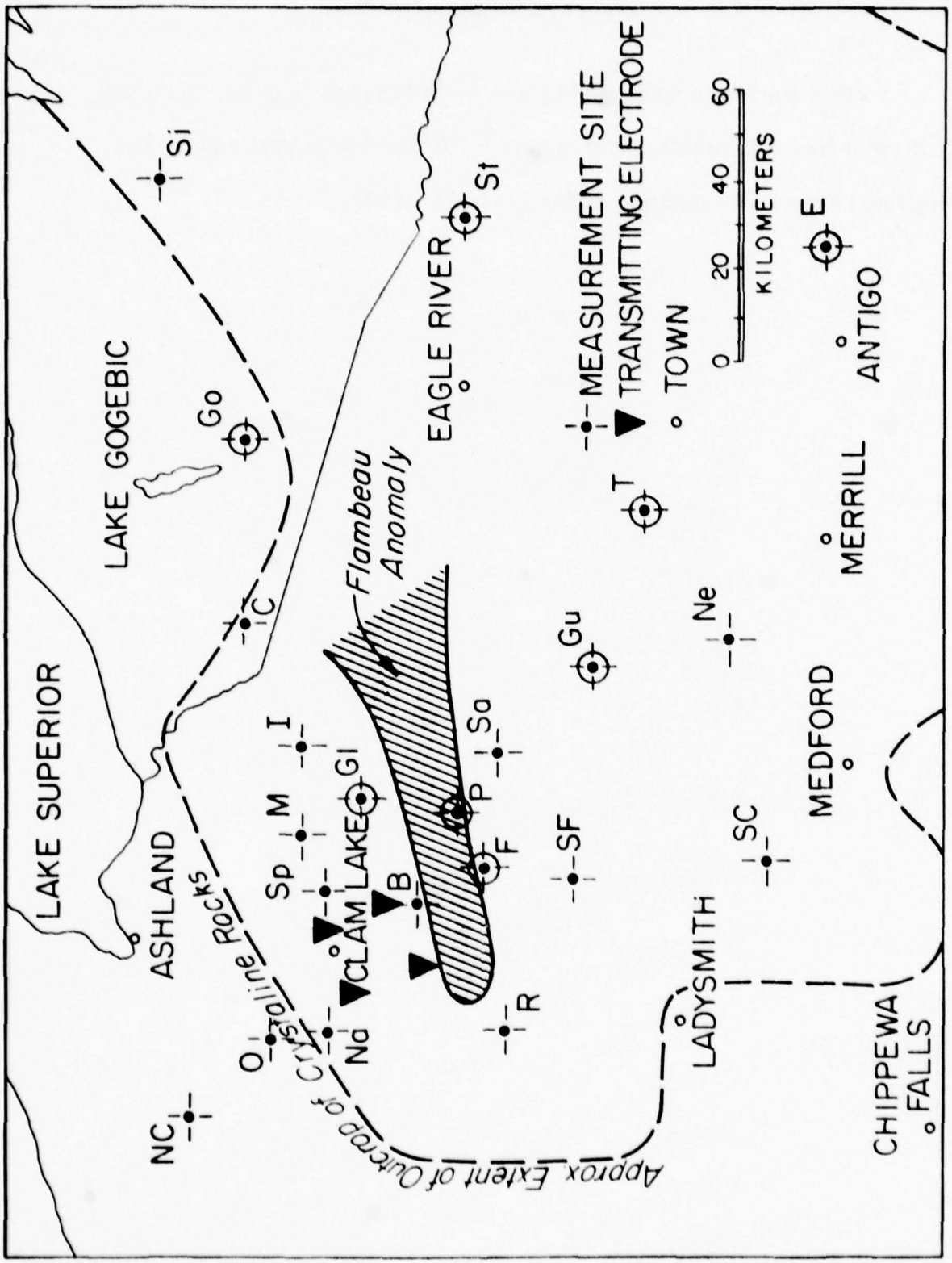

Figure 1 WTF Antennas and Measurement Site Locations

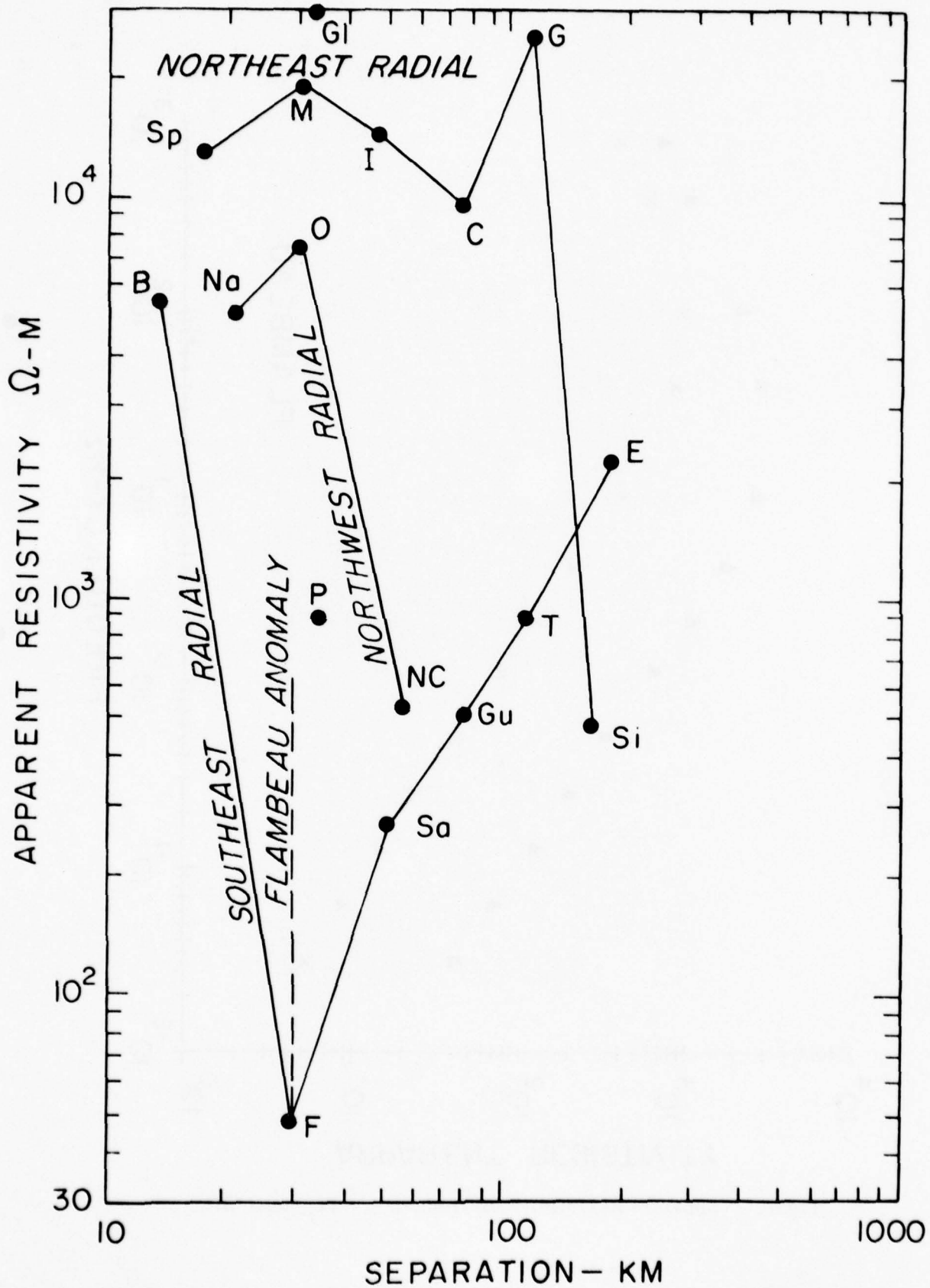

Figure 2 DC Dipole-Dipole Apparent Resistivity vs Dipole Separation

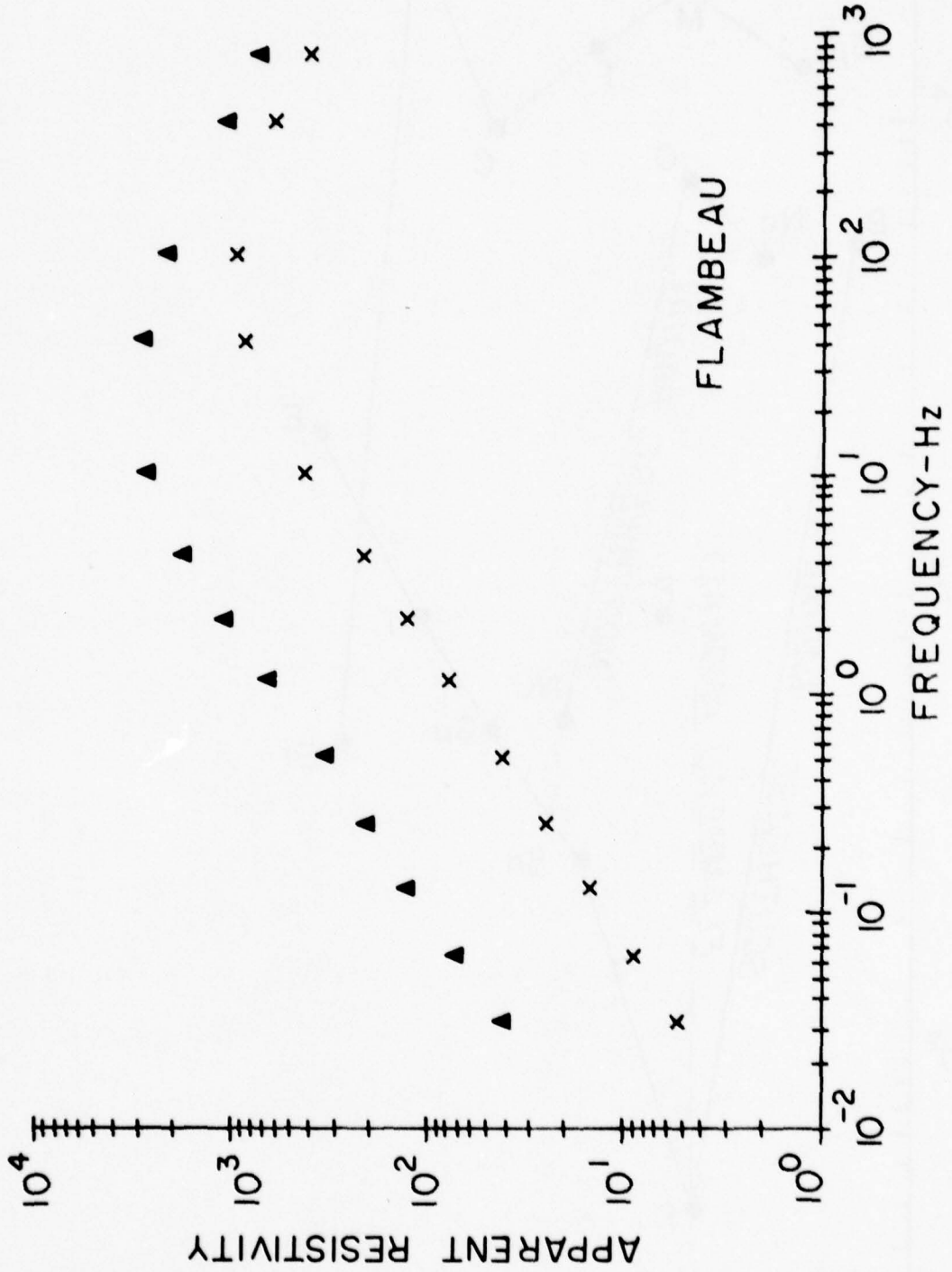

Figure 3 Apparent Resistivity vs Frequency - Flambeau Site

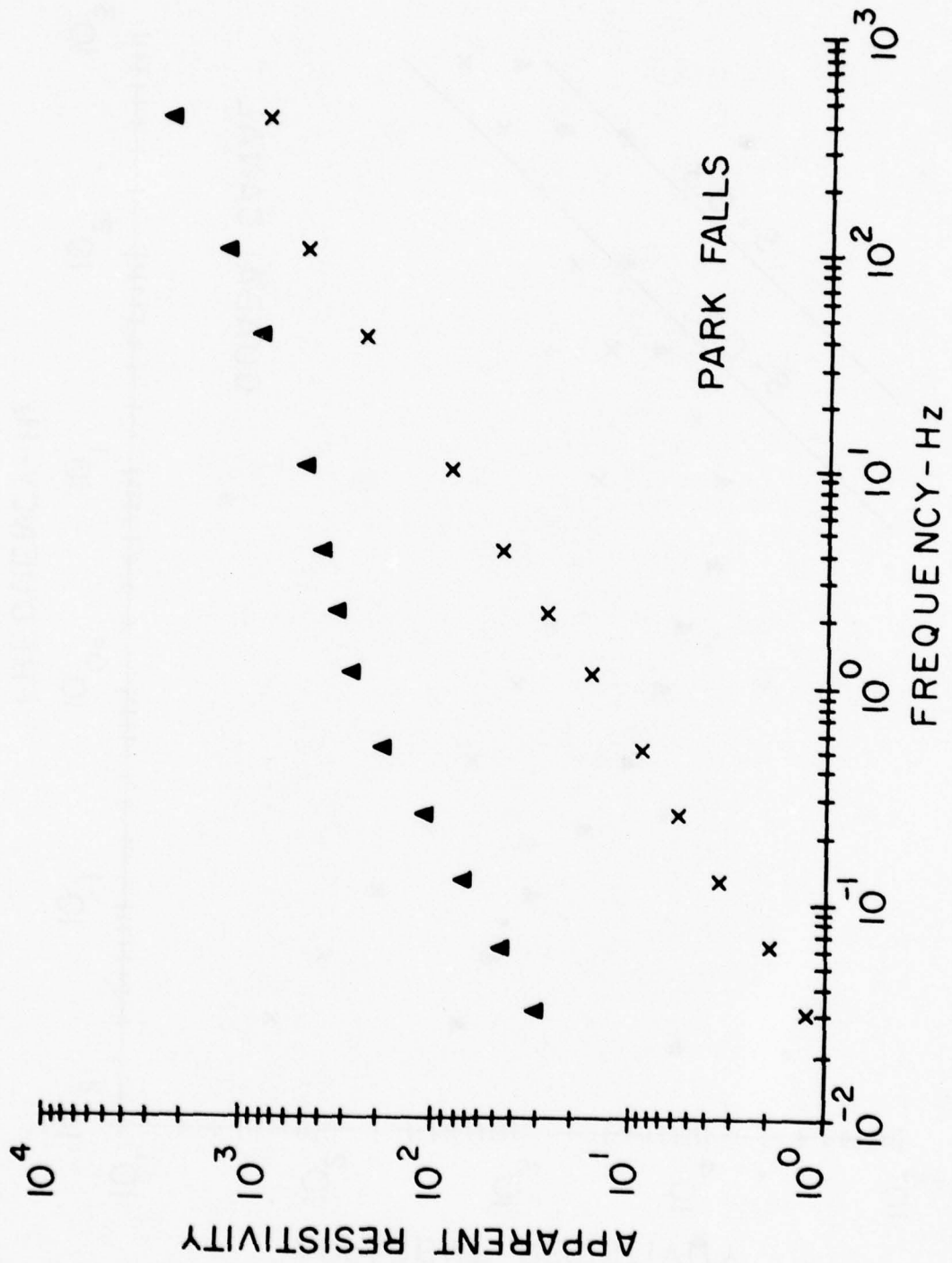

Figure 4 Apparent Resistivity vs Frequency - Park Falls Site

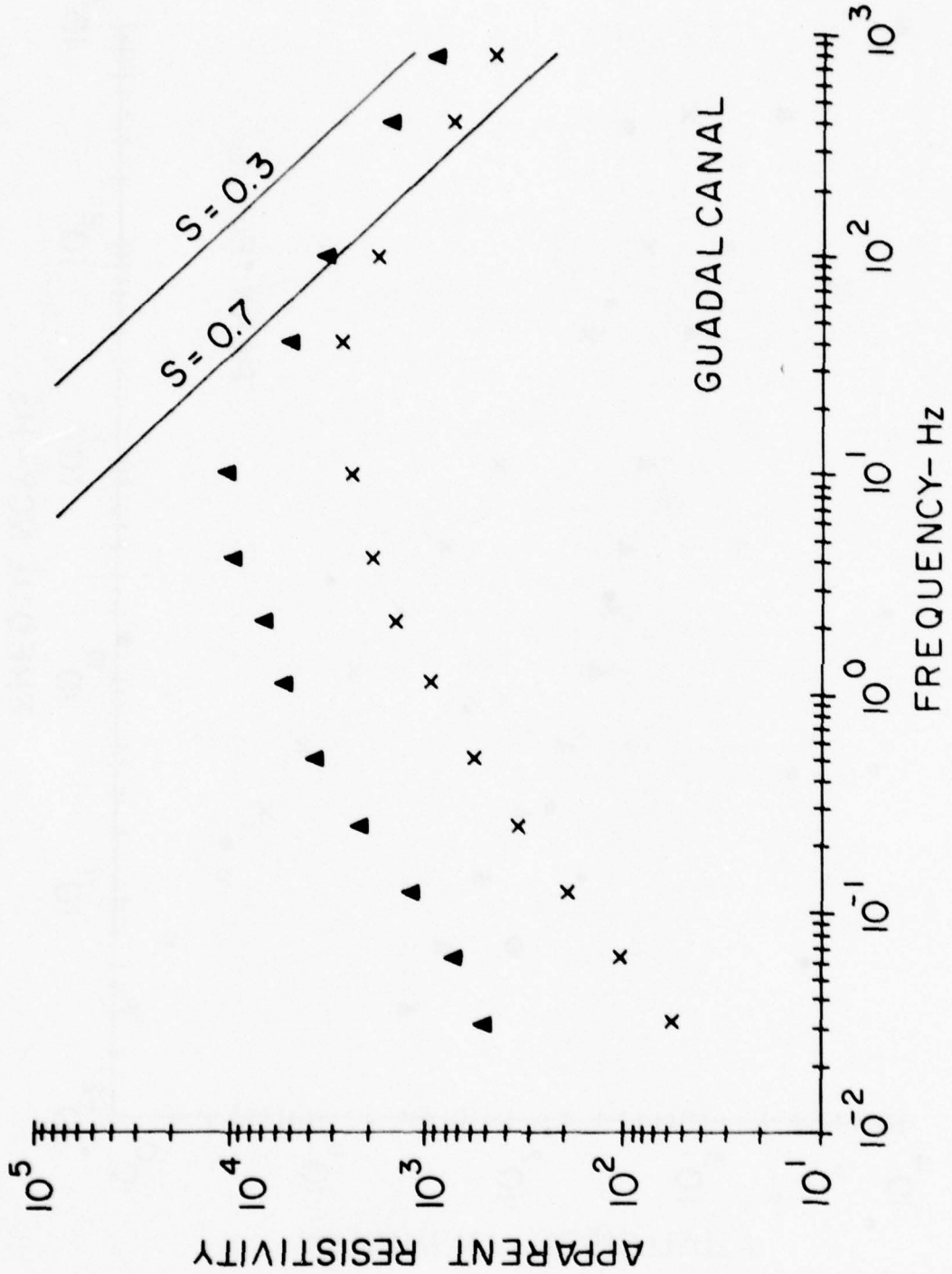

Figure 5 Apparent Resistivity vs Frequency - Guadalcanal Site

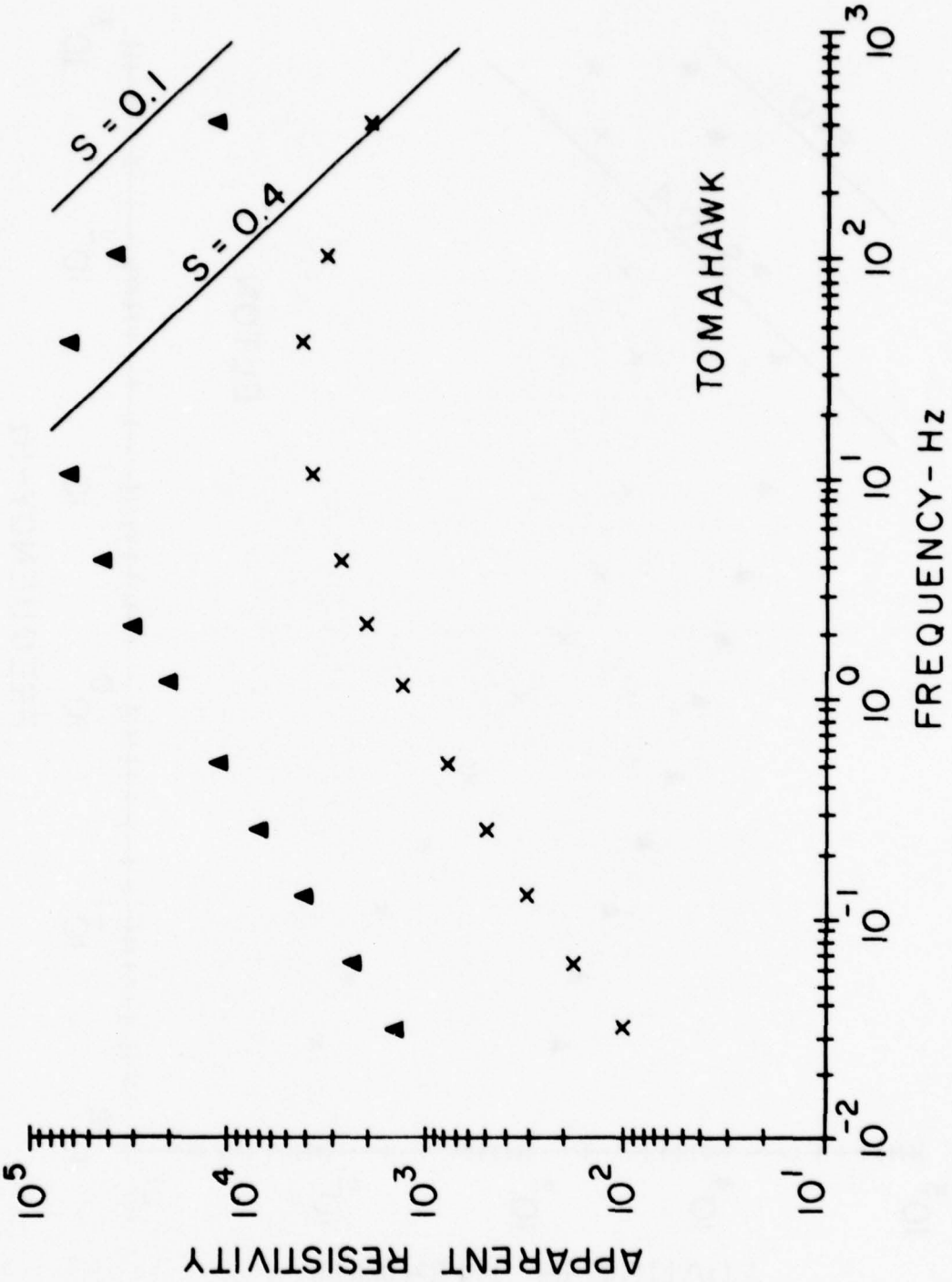

Figure 6 Apparent Resistivity vs Frequency - Tomahawk Site

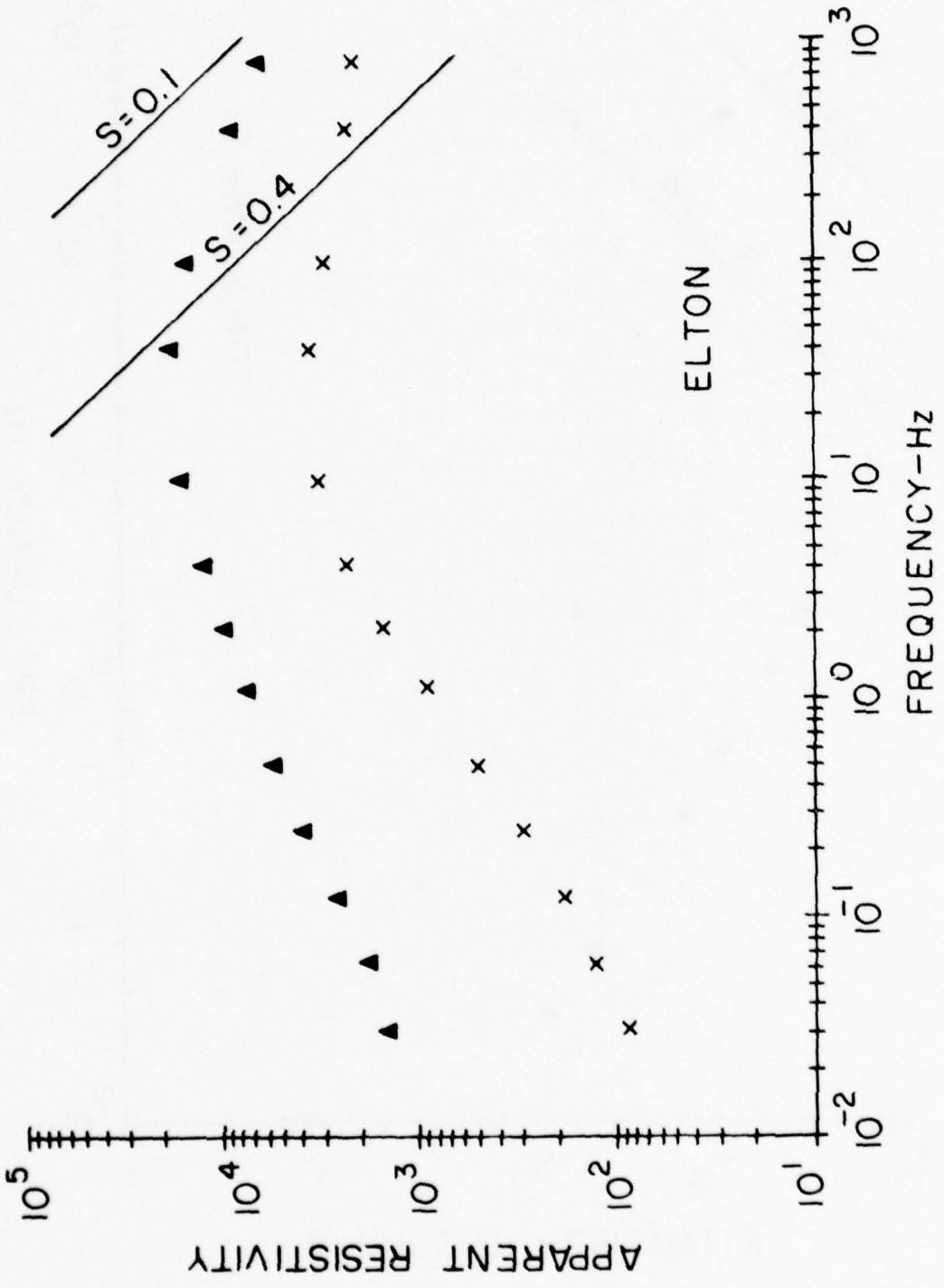

Figure 7 Apparent Resistivity vs Frequency - Elton Site

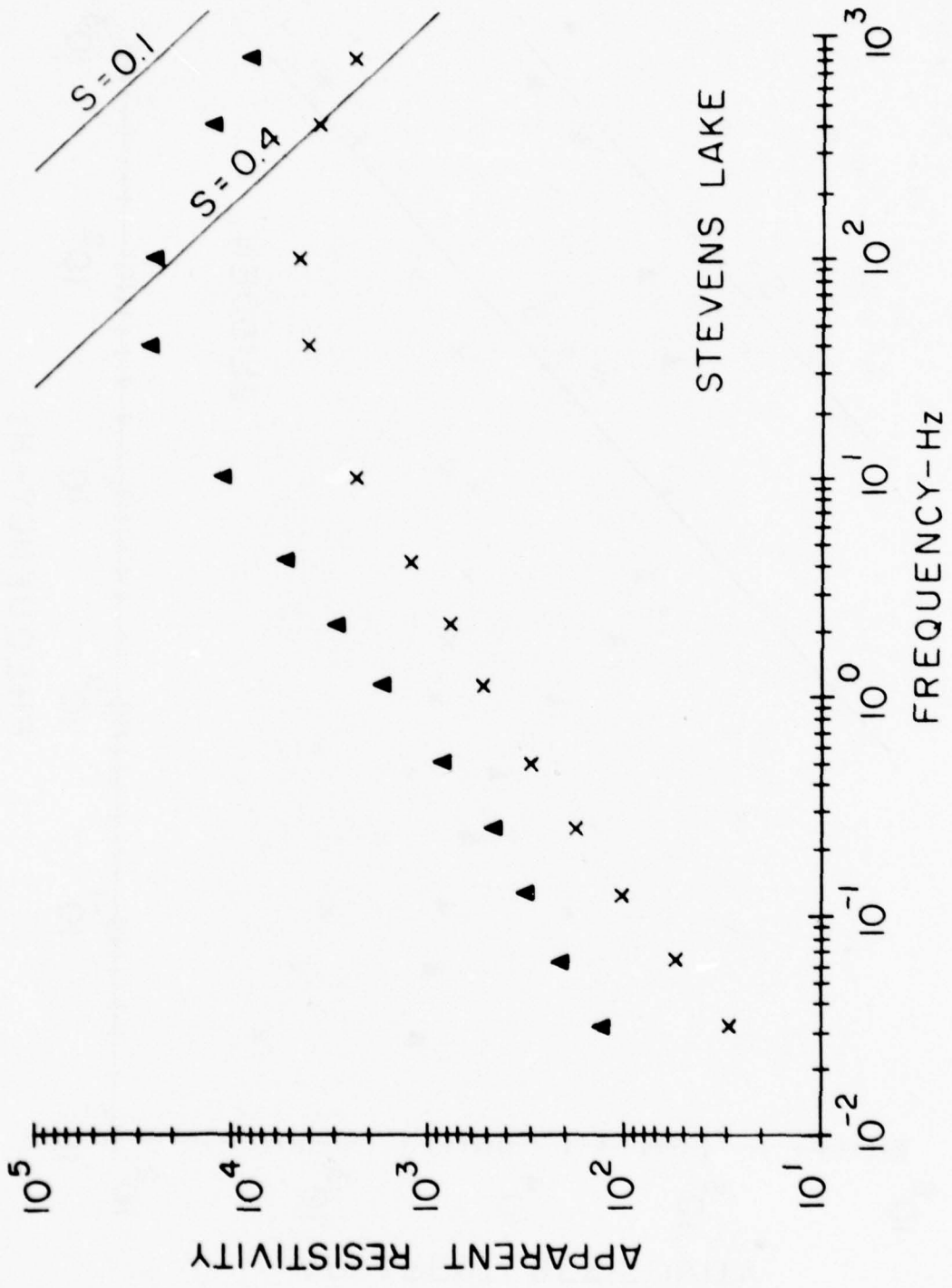

Figure 8 Apparent Resistivity vs Frequency - Stephens Lake Site

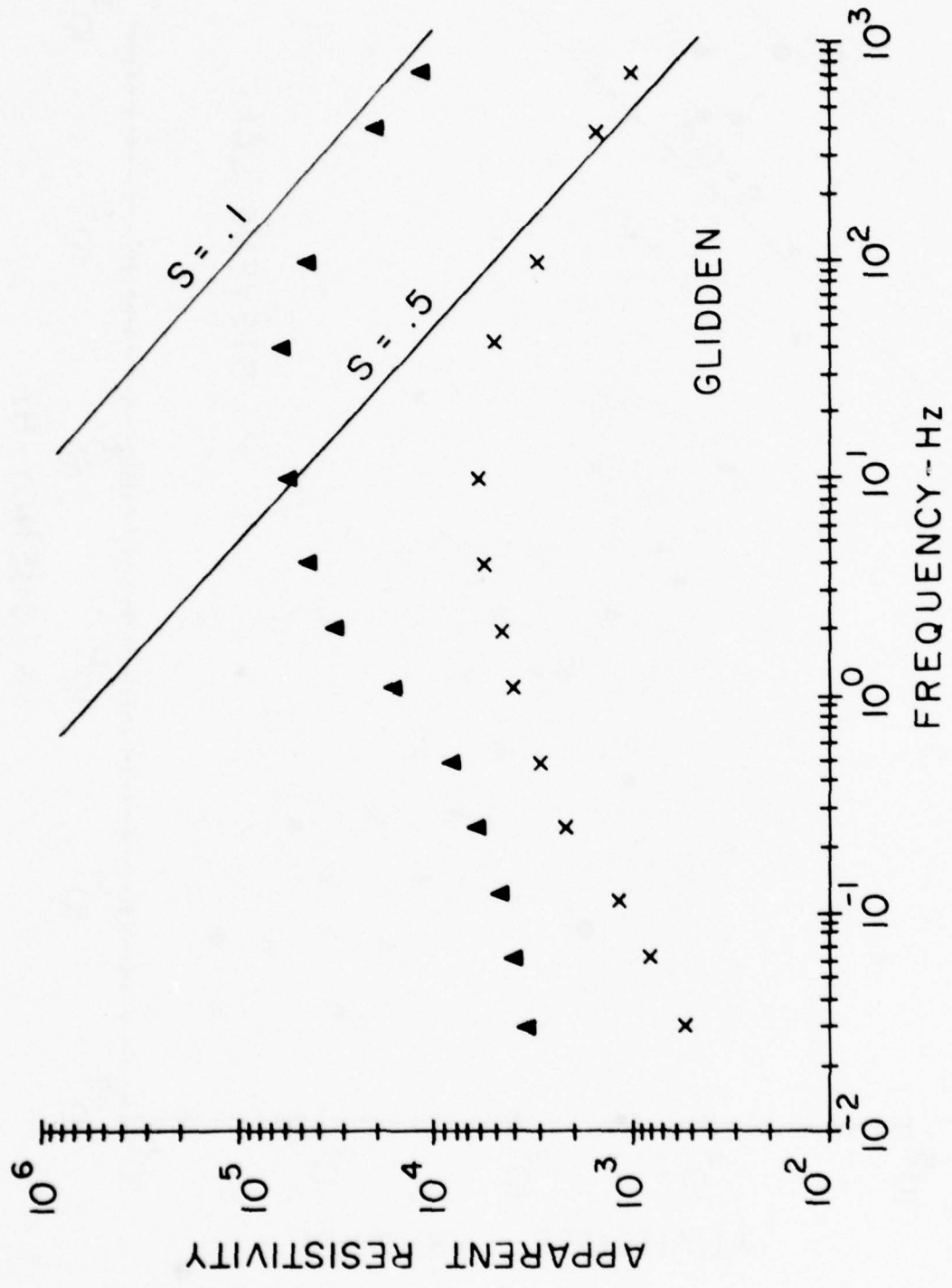

Figure 9 Apparent Resistivity vs Frequency - Glidden Site

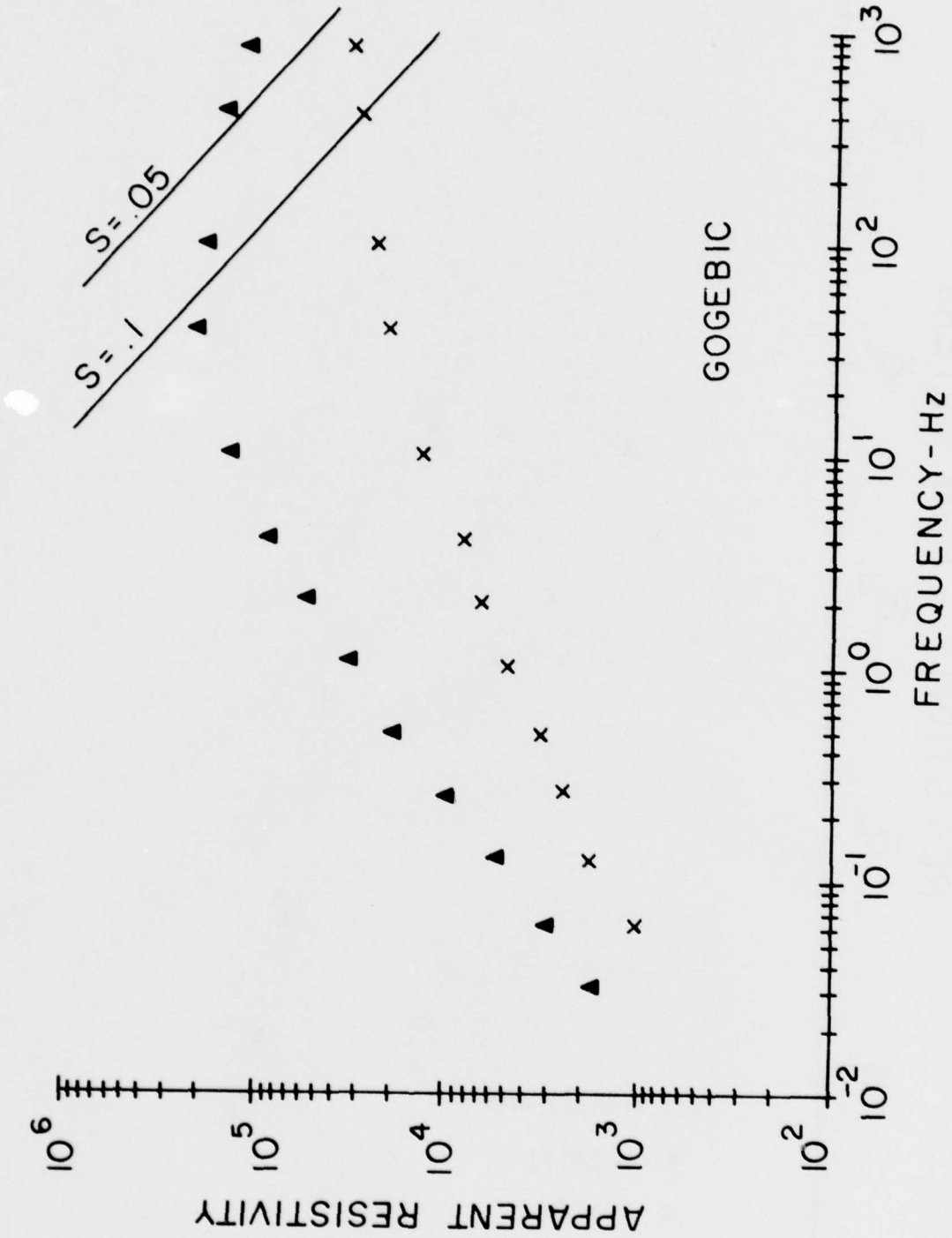

Figure 10 Apparent Resistivity vs Frequency - Gogebic Site

Figure 11 Resistivity - Depth Sounding - Flambeau Site

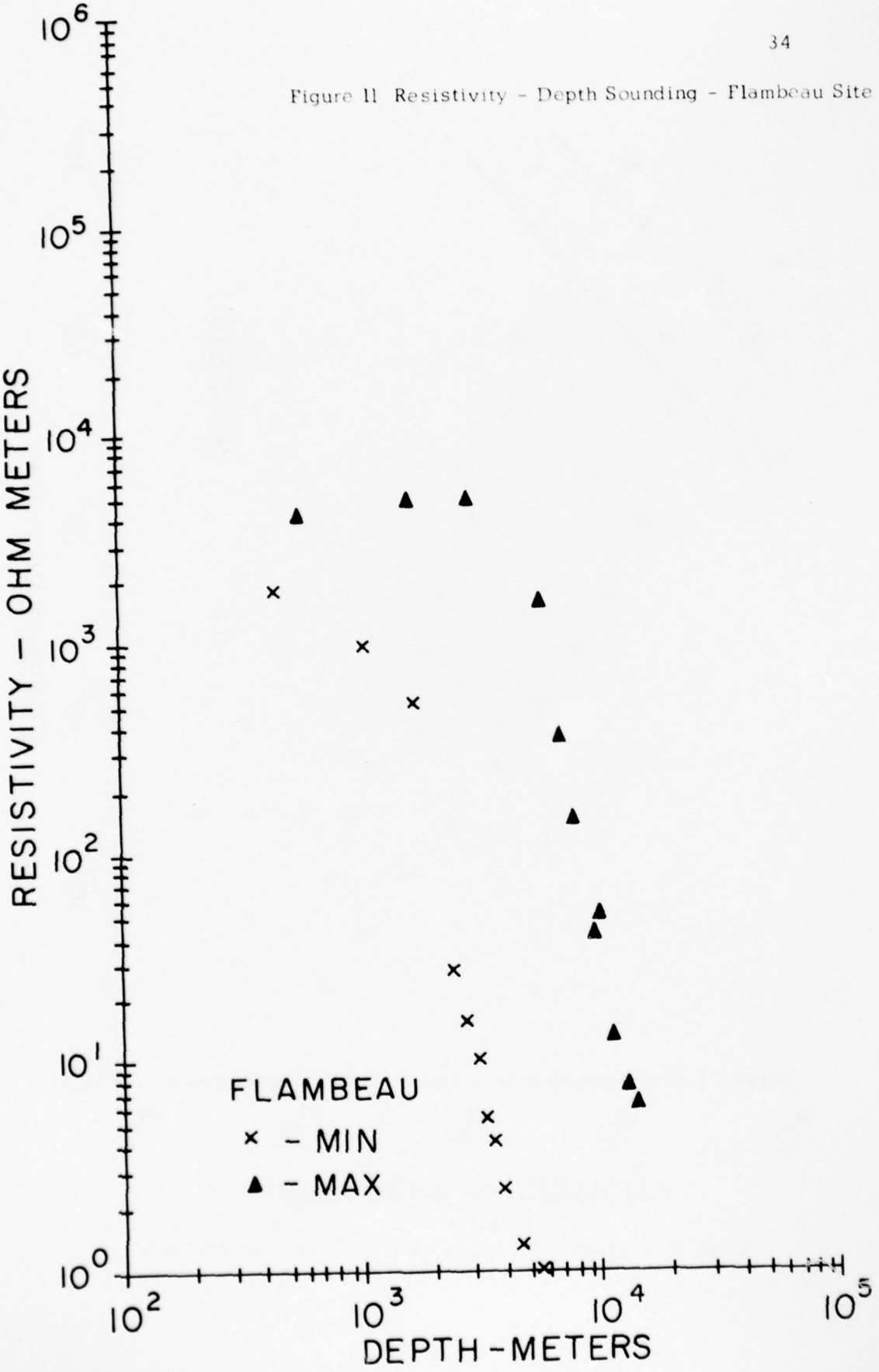

Figure 12 Resistivity - Depth Sounding
Park Falls Site

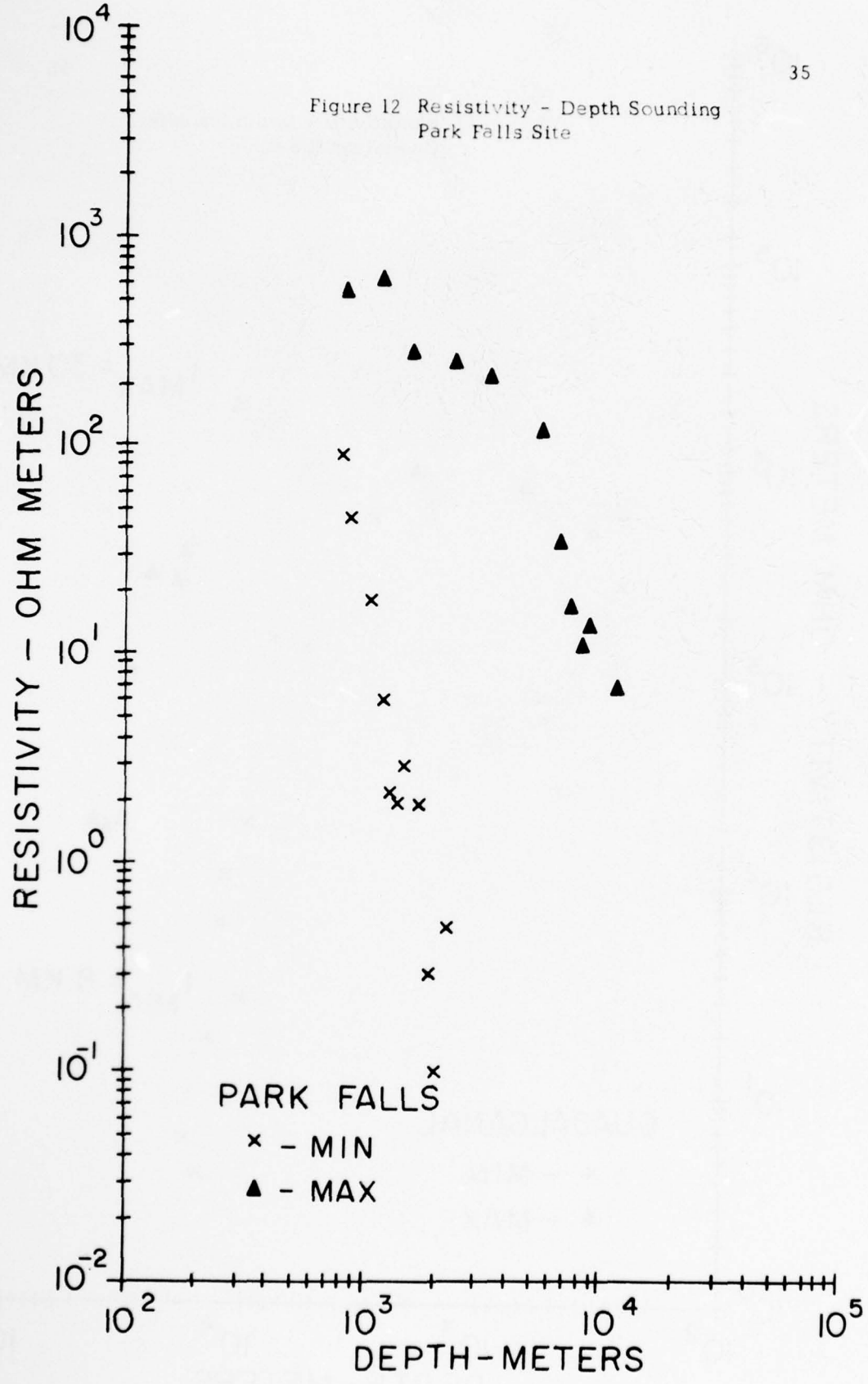

Figure 13 Resistivity - Depth Sounding
Guadalcanal Site

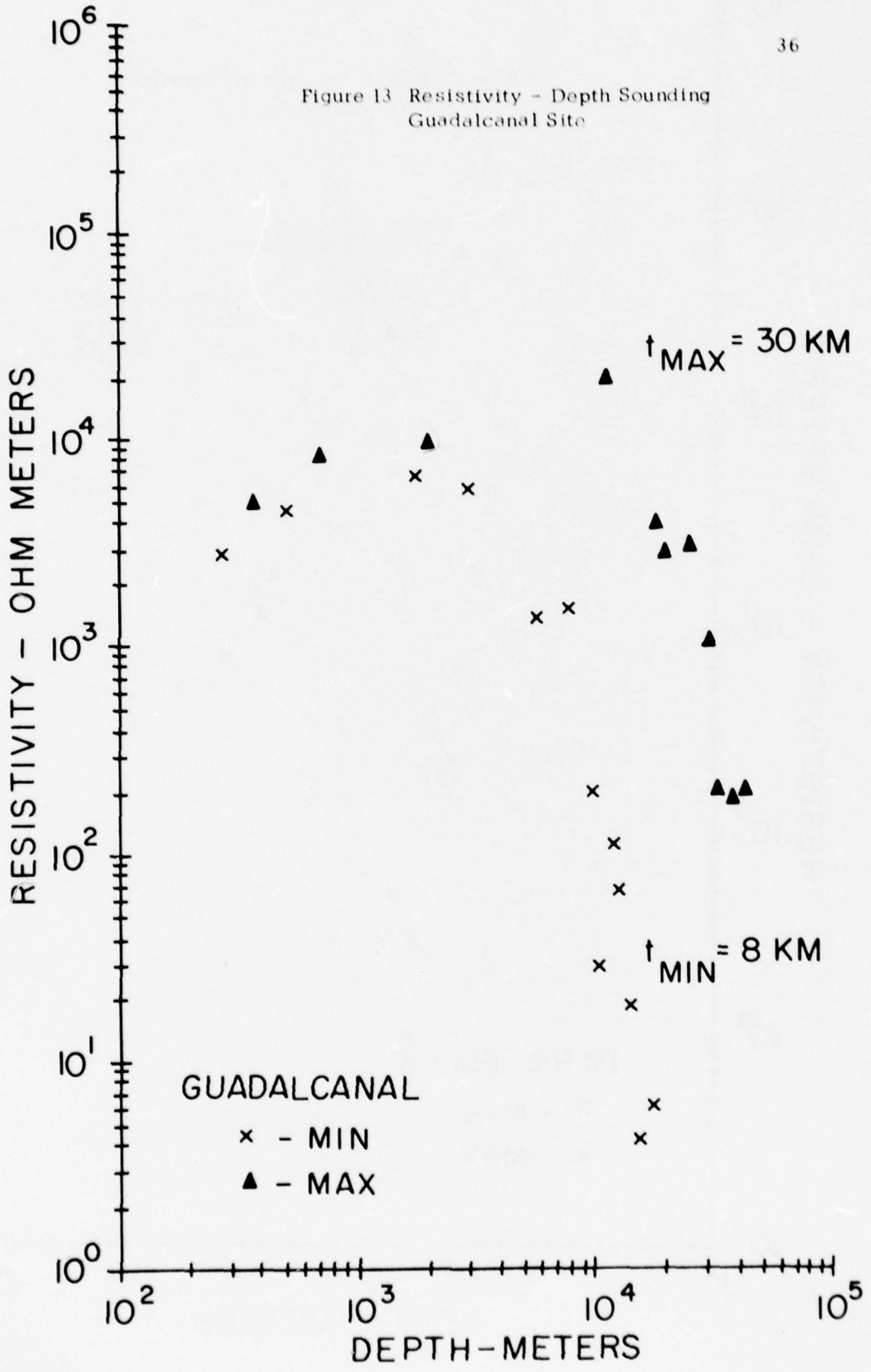

Figure 14 Resistivity - Depth Sounding
Tomahawk Site

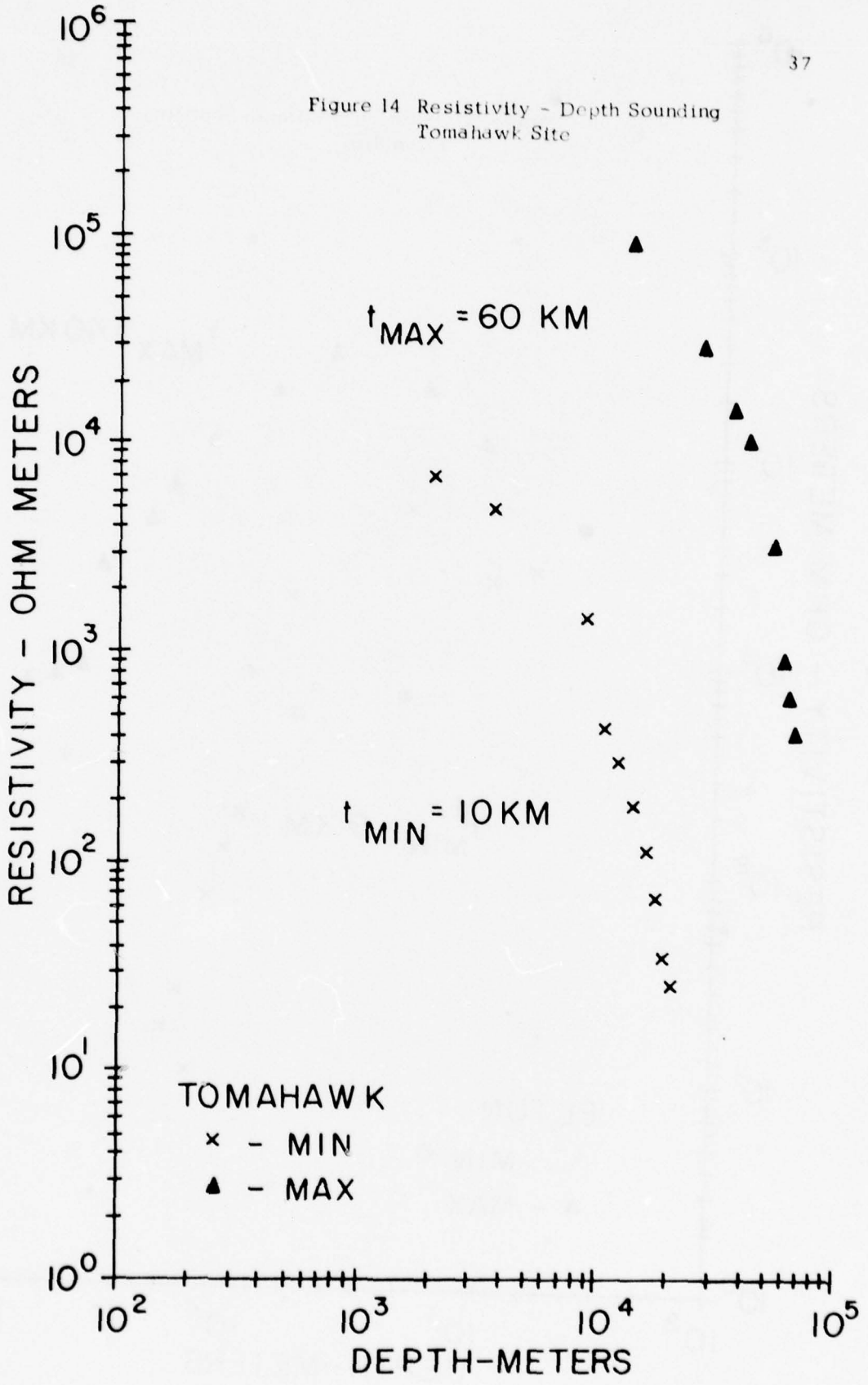

Figure 15 Resistivity - Depth Sounding
Elton Site

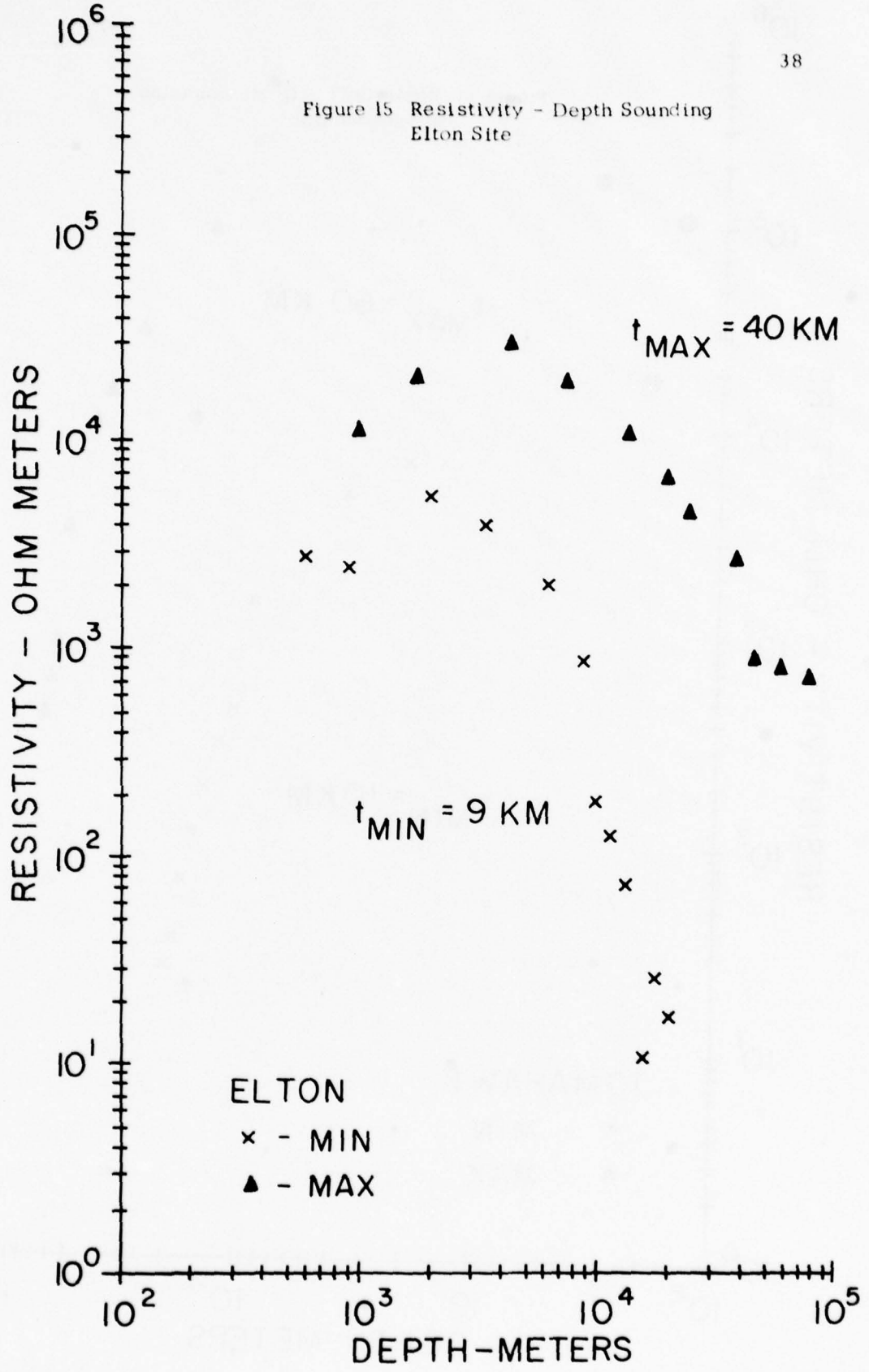

Figure 16 Resistivity - Depth Sounding
Stephens Lake Site

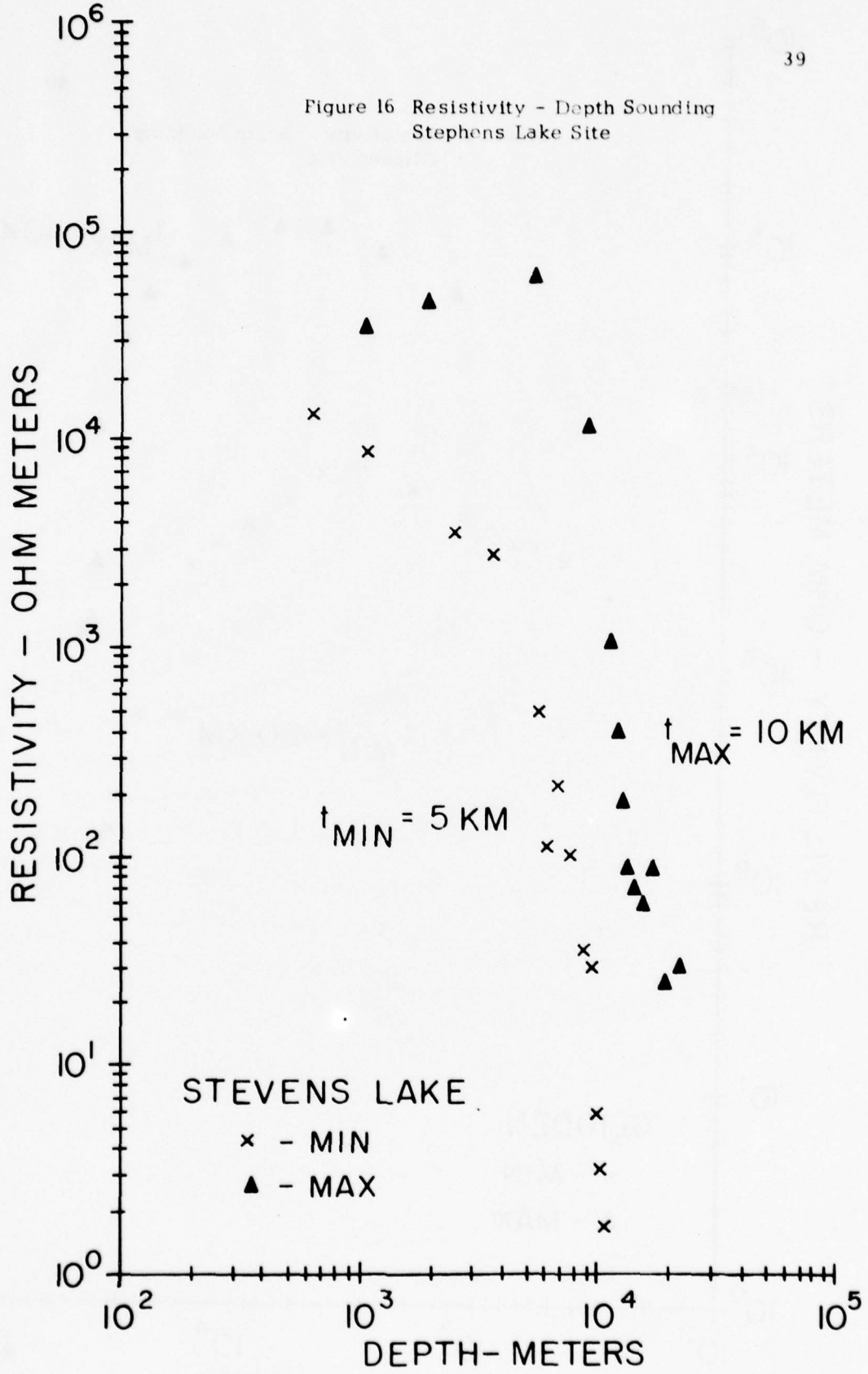

Figure 17 Resistivity - Depth Sounding
Glidden Site

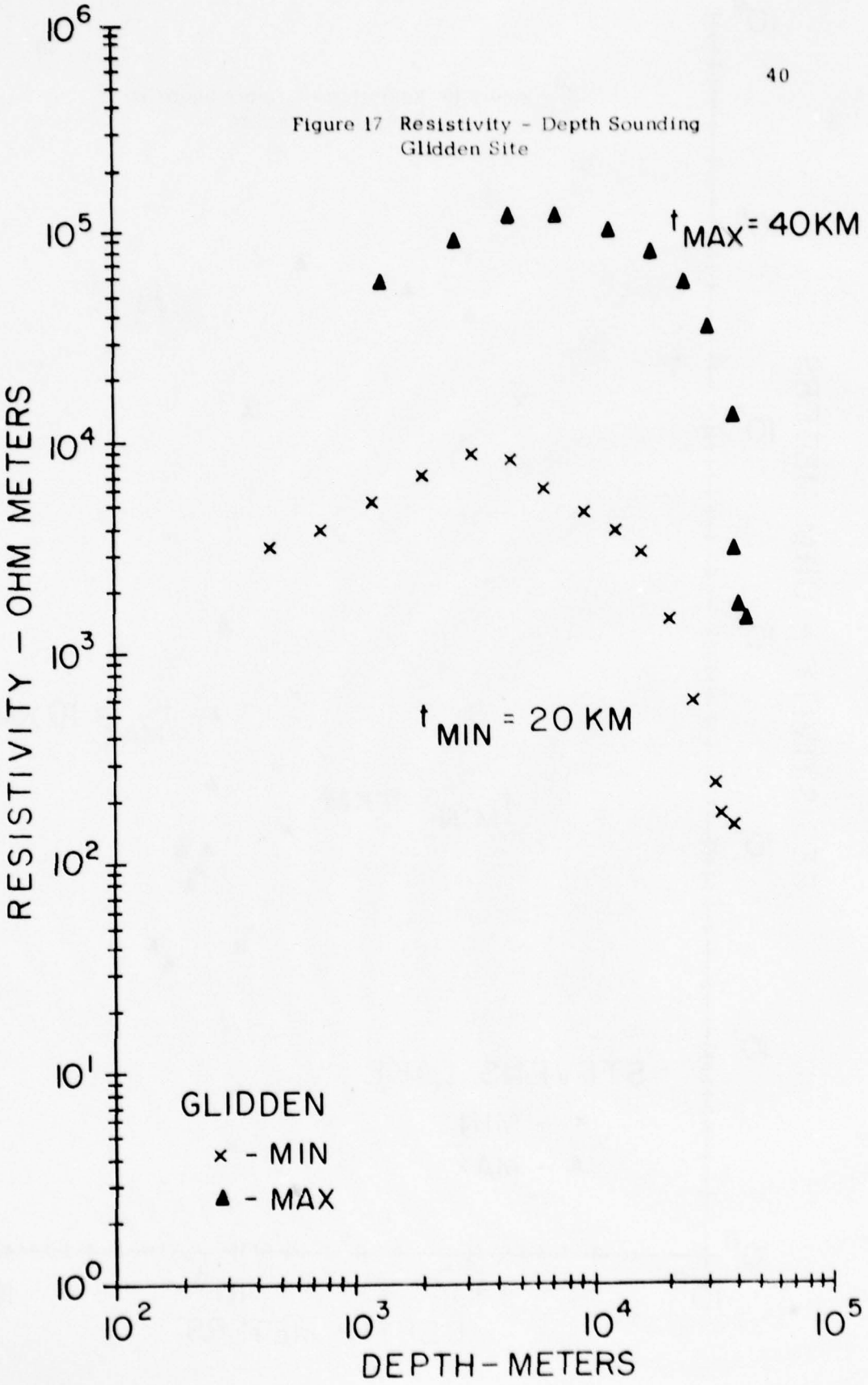

Figure 18 Resistivity - Depth Sounding
Gogebic Site

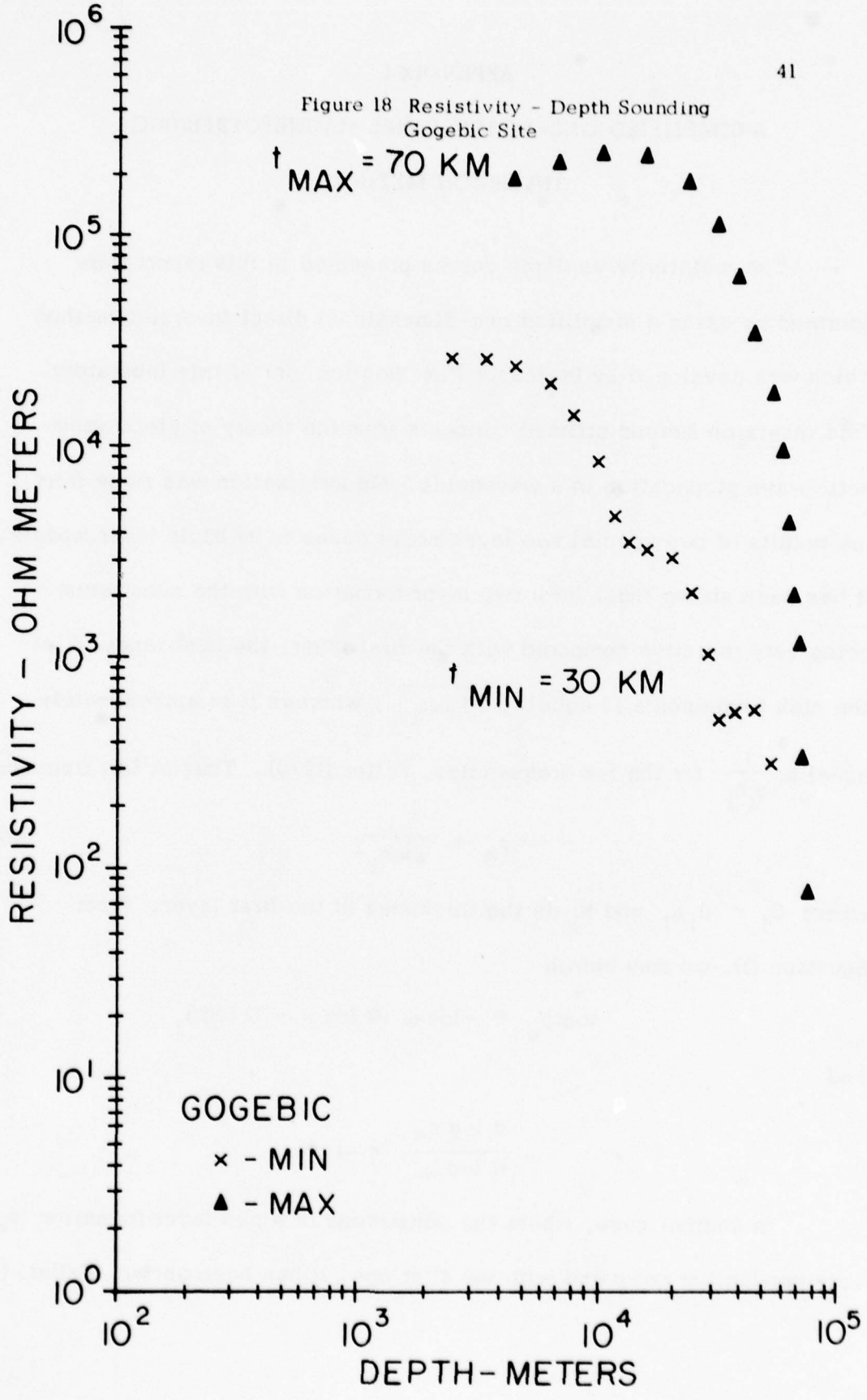

APPENDIX I

A SIMPLIFIED ONE-DIMENSIONAL MAGNETOTELLURIC INVERSION METHOD

The resistivity vs depth curves presented in this report were obtained by using a simplified one-dimensional direct inversion method which was developed by Professor F.X. Bostick, Jr. of this laboratory. This inversion method utilized concepts from the theory of electromagnetic wave propagation in a waveguide. Generalization was made from the results of two special two layer model cases to multiple layer models. It has been shown that, for a two layer formation with the substratum being very resistive compared with the first layer, the impedance Z at the high frequencies is equal to $\sqrt{j\mu\omega\rho_1}$, whereas it is approximately equal to $\frac{1}{\sigma_1 h_1}$ for the low frequencies, Keller (1970). Thus at low frequencies

$$\rho_a \cong \frac{1}{\omega\mu S_1^2} \tag{1}$$

where $S_1 = \sigma_1 h_1$ and h_1 is the thickness of the first layer. From Equation (1), we may obtain

$$\log \rho_a \cong -\log \omega - \log \mu - 2 \log S_1 \tag{2}$$

and

$$\frac{d \log \rho_a}{d \log \omega} \cong -1 \tag{3}$$

In another case, where the substratum of a two layer formation is very conductive compared with the first one, it has been shown, Keller, (1973)

that at high frequencies $\rho_a = \rho_1$ and at low frequencies

$$\rho_a \cong \omega \mu h_1^2 \tag{4}$$

From Equation (4) we obtain

$$\log \rho_a \cong \log \omega + \log \mu + \log h_1^2 \tag{5}$$

and

$$\frac{d \log \rho_a}{d \log \omega} \cong 1 \tag{6}$$

These approximations lead to an apparent resistivity $\log \rho_a$ curve which is a smooth function of $\log \omega$ and the derivative of the $\log \rho_a$ with respect to $\log \omega$ has an absolute value less than or equal to 1, that is,

$$\left| \frac{d \log \rho_a}{d \log \omega} \right| \leq 1$$

for any horizontal layered model.

Equations (2) and (5) may be combined to obtain the following equation which generates resistivity distribution ρ as a function of depth.

$$\rho = \rho_a \frac{1 - \frac{d \log \rho_a}{d \log \omega}}{1 + \frac{d \log \rho_a}{d \log \omega}} \tag{7}$$

The corresponding depth is

$$D = \left(\frac{\rho_a}{\omega \mu} \right)^{\frac{1}{2}} \tag{8}$$

Equations (7) and (8) together give an estimation of the one-dimensional resistivity (or conductivity) distribution.

Since the apparent resistivity is the average resistivity over depth,

we expect $\log \rho_a$ to be a smooth function of $\log \omega$. In cases where the data are contaminated by noise there will be scatter in the $\log \rho_a$ vs $\log \omega$ curve. Often the application of Equation (7) requires that smoothing techniques be performed on the $\log \rho_a$ vs $\log \omega$ curves before inversion is made. Recently Professor F.X. Bostick, Jr., and John E. Boehl, of this Laboratory have devised a smoothing technique which is based on the fact that the phase of the apparent resistivity estimate can also be used to determine the magnitudes of the apparent resistivities if a minimum phase condition is reasonably well satisfied for the data under consideration. Through the Hilbert Transform the slope of the magnitude of the apparent resistivity at each point may be obtained from the phase. The level of the curve is determined by a least square fit with the magnitude of the original log apparent resistivity curve, with a weighting constant given to each point according to the statistical confidence calculated for that point. This smoothing technique was used in this report to smooth the apparent resistivity curves before the inversion was carried out. The details of the process are given in Appendix II.

APPENDIX II

PHASE SMOOTHING

Noise is inevitably encountered throughout the MT data acquisition and analysis process. As a result of this noise, the calculated values of apparent resistivity in the principal directions will be biased from their true values. The direction of this bias is predictable if it is known whether the predominant noise has been introduced on the E or H channel, Sims, et al, (1971). In this case, the particular estimate of Z which is insensitive to the suspected type of noise may be chosen for apparent resistivity calculations.

Often, however, noise is present on both the E and H channels and so regardless of which estimates are used some scatter will result in the apparent resistivity vs. frequency data. A natural step in the MT analysis process then is to fit a smooth function of frequency through the calculated results. Rather than arbitrarily constructing such a curve by hand, an analytic method has recently been used with success. This smoothing process invokes the theory of the Hilbert Transform under the constraint of minimum phase. If the MT impedance function exhibits the property of minimum phase, the phase information of Z as well as the magnitude of Z may then be used to better define the true apparent resistivity curve.

Following is a brief outline of the derivation of the formulas used to smooth the apparent resistivity curve through the impedance phase information.

If it is assumed that the MT impedance function $Z(\omega)$ is minimum phase and is written as

$$Z(\omega) = |Z(\omega)| e^{j\phi(\omega)}$$

then, through the Hilbert Transform, a theorem of Bode (1945), which relates amplitude and phase at radian frequency ω_o is given by

$$\phi(\omega_o) = \frac{1}{\pi} \int_{-\infty}^{\infty} \left[\frac{d(\ln |Z|)}{d(\ln \omega)} \right] \ln \coth \frac{|u|}{2} \, du \qquad (1)$$

where $u = \ln \frac{\omega}{\omega_o}$.

For ease of notation define

$$y = \ln \omega \qquad \text{and} \qquad s(y) = \frac{d(\ln |Z|)}{d(\ln \omega)}$$

and also let $$f(y_o - y) = \ln \coth \frac{|y - y_o|}{2} \, .$$

Then Equation (1) is written as

$$\phi(y_o) = \frac{1}{\pi} \int_{-\infty}^{\infty} s(y) \, f(y_o - y) \, dy \qquad (2)$$

The Fourier Transform of this convolution is

$$\Phi(x) = \frac{1}{\pi} S(x) F(x) \tag{3}$$

From a table of integrals

$$\int_{-\infty}^{\infty} \ln \coth \frac{|u|}{2} du = \frac{\pi^2}{2} \tag{4}$$

Using this identity, Equation (2) may be rearranged to give

$$s(y_o) = \frac{2}{\pi} \phi(y_o) + \frac{2}{\pi^2} \int_{-\infty}^{\infty} \left| s(y_o) - s(y) \right| f(y_o - y)\, dy \quad . \tag{5}$$

The function $f(y_o - y)$ dies off rapidly away from the point $y=y_o$ so that the major contribution of the integral portion of (5) lies about this point. If the slope of the amplitude of $|Z|$ varies slowly enough in the vicinity of $y=y_o$ then the slope is very nearly defined by the first order term

$$s(y_o) = \frac{2}{\pi} \phi(y_o) \tag{6}$$

In this case, Equation (6) may be integrated to give the magnitude of $|Z|$ function in terms of the phase

$$\ln |Z| = \frac{2}{\pi} \int \phi(y)\, dy + C \tag{7}$$

where C is the constant of integration and represents the quantity to be added point by point to $|Z|$ on a log scale.

The constant in Expression (7) is evaluated by adjusting the level of the integral part of this Equation on a log $|Z|$ scale until a least square fit of the phase-derived $|Z|$ is achieved with the original data. Thus, both amplitude and phase data of the impedance estimate are used to determine the smoothed version of the $|Z|$ curve.

If the slope of log $|Z|$ on a log ω scale does not vary slowly enough, then the second order term of Equation (5) must be included in the smoothing process. Let this second order term be defined as

$$\xi(y_o) = \frac{2}{\pi^2} \int_{-\infty}^{\infty} [s(y_o) - s(y)]\, f(y_o - y)\, dy \tag{8}$$

which with the integral identity (4) becomes

$$\xi(y_o) = s(y_o) - \frac{2}{\pi^2}\, s(y) * f(y)$$

where * represents a convolution. The Fourier Transform of the second order term is then

$$\psi(x) = S(x) \left[1 - \frac{2}{\pi^2}\, F(x) \right] \tag{9}$$

where $\psi(x)$ represents the Fourier Transform of $\xi(y)$, etc. By combining Equations (3) and (9) the second order term is then

$$\xi(y_o) = \pi \mathcal{F}^{-1} \left\{ \psi(x) \left[\frac{1}{F(x)} - \frac{2}{\pi^2} \right] \right\} \tag{10}$$

where $\mathcal{F}^{-1}\{\ \}$ denotes the inverse Fourier Transform. It can furthermore be shown that the Fourier Transform of the ln coth convolver function is

$$F(x) = \frac{\pi^2}{2}\left[\frac{\tanh\left(\frac{\pi x}{2}\right)}{\left(\frac{\pi x}{2}\right)}\right] \tag{11}$$

The slope of log $|Z|$ on a ln ω scale is then fully given by combining (5), (8), (10), and (11) to give

$$\frac{d\,(\ln|Z|)}{d\,(\ln\omega)} = \frac{2}{\pi}\,\phi\,(\ln\omega) + \frac{2}{\pi}\,\mathcal{F}^{-1}\left|T(x)\,\Phi\,(x)\right| \tag{12}$$

where the convolving function $T(x)$ of the second order term is

$$T(x) = \frac{\left(\frac{\pi x}{2}\right)}{\tanh\left(\frac{\pi x}{2}\right)} - 1 \quad .$$

The MT impedance function $|Z|$ may then be obtained from Equation (12) in the same manner as was done with the first order term outlined following expression (6).

In the process of analysis it is often more convenient to smooth the apparent resistivity curve rather than the magnitude of impedance. This can be accomplished through the substitution in the preceding discussion

$$\rho_A = \frac{1}{\omega\mu}\,|Z|^2 \quad .$$

Then

$$\ln \rho_A = 2 \ln |Z| - \ln \omega + \text{constant}$$

and

$$\frac{d\left(\ln \rho_A\right)}{d\,(\ln \omega)} = 2 \frac{d\,(\ln |Z|)}{d\,(\ln \omega)} - 1$$

so that

$$\frac{d\,(\ln |Z|)}{d\,(\ln \omega)} = \frac{1}{2}\left[\frac{d\left(\ln \rho_A\right)}{d\,(\ln \omega)} - 1\right] \tag{13}$$

Substitution of (13) into (12) finally yields

$$\frac{d\left(\ln \rho_A\right)}{d\,(\ln \omega)} = \left[\frac{4}{\pi} \phi\,(\ln \omega) - 1\right] + 2\,\xi\,(\ln \omega) \tag{14}$$

where the second order term $\xi(y)$ is defined as before in relation (10). The apparent resistivity vs frequency curve may finally be obtained by integrating Equation (14)

$$\rho_A = \int \left[\frac{4}{\pi} \phi - 1\right] d\,(\ln \omega) + 2 \int \xi\, d\,(\ln \omega) + C$$

where the constant C may be evaluated by a least square fit between the curve resulting from the integration and the original ρ_A data.

In some cases, the phase of Z varies slowly enough with log frequency so that the first integral is sufficient for the definition of ρ_A. In these instances, the computation is greatly simplified and may be performed without the aid of a computer.

REFERENCES

Berdichevskiy, M.N., Electrical exploration with the magneto-telluric profiling method, Nedra, Moscow, 255 pp, 1968.

Bode, H.W., Network analysis and feedback amplifier design, D. Van Nostrand, New York, 1945.

Bostick, F.X., Jr., and H.W. Smith, Investigation of large-scale inhomogeneities in the earth by the magnetotelluric method, Proc. IRE, 40(11), p. 2339-2346, 1962.

Bostick, F.X., Jr., A simple almost exact method of MT analysis, "Workshop on Evaluation of Electrical Methods in the Geothermal Environment," (WEEMGE). Snowbird, Utah, November 1976. University of Utah Report - Geothermal Workshop, Jan 1977.

Cagniard, L., Basic theory of the magnetotelluric method of geophysical prospecting, Geophysics, Vol. 18, p. 605-635, 1953.

Cantwell, T., Detection and analysis of low-frequency magnetotelluric signals, Ph.D. Thesis, MIT, 1960.

Cantwell, T., and T.R. Madden, Preliminary report on crustal magnetotelluric measurements, J. Geophys. Res., 65 (12), p. 4202-4205, 1960.

Davidson, D., D.N. Macklin, and K. Vozoff, Resistivity surveying as an aid in Sanguine site selection, IEEE Transactions on Communications, Vol. Com-22, no. 4, p. 389, 1974.

Dowling, F.L., Magnetotelluric measurements across the Wisconsin Arch, J. Geophys. Res., vol. 75, no. 14, p. 2683-2689, 1970.

Hermance, J.F., Processing of magnetotelluric data, Phys. of Earth and Planetary Interiors, vol. 7, p. 349-364, 1973.

Keller, G.R., Dipole method for deep resistivity studies, Geophysics, vol. 51, no. 6, p. 1088-1104, 1966.

Keller, G.V., Electrical properties of the earth's crust, A survey of the literature, ONR Contract Number N000-14-70-C-0290, 1970.

Keller, G.V., and R.B. Furgerson, Determining the resistivity of a resistant layer in the crust, to appear in AGU Monograph No. 20, "The Nature and Physical Properties of the Earth's Crust," 1977.

Sims, W.E., F.X. Bostick, Jr., and H.W. Smith, The estimation of magnetotelluric impedance tensor elements from measured data, Geophysics, vol. 36, no. 5, p. 938-942, 1971.

Stanley, W.D., J.E. Boehl, F.X. Bostick, Jr., and H.W. Smith, Geothermal significance of magnetotelluric soundings in the snake river plain - yellowstone region, accepted for publication in the J. Geophys. Res.

Sternberg, B.K., and C.S. Clay, Flambeau anomaly - a high conductivity anomaly in the southern extension of the Canadian shield, to appear in AGU Monograph No. 20, "The Nature and Physical Properties of the Earth's Crust," 1977.

Swift, C.M. Jr., A magnetotelluric investigation of an electrical conductivity anomaly in the southwestern United States, Ph.D. Thesis, MIT, 1967.

Vozoff, Keeva, The Magnetotelluric method in the exploration of sedimentary basins, Geophysics, vol. 37, no. 1, p. 98-141, 1972.

Wait, J.R., Theory of magnetotelluric field, Radio Sci., 66 D(5), p. 509-541, 1962.

Word, D.R., H.W. Smith, and F.X. Bostick, Jr., Crustal investigations by the magnetotelluric tensor impedance method, Geophysical Monograph Series, vol. 14, The structure and physical properties of the earth's crust, John G. Heacock, editor, American Geophysical Union, 1971.

DISTRIBUTION LIST

for

FINAL REPORT CONTRACT N00014-76-C-0484

Mr. M. Kraichman
Code WR 43
Naval Surface Weapons Center
(White Oak)
Silver Spring, MD 20910

Dr. John R. Davis, Code 5460
Naval Research Laboratory
Washington, DC 20390

Dr. Jaap Boosman
Chief of Naval Operations (OP 987P1)
Pentagon, Room 4B513
Washington, DC 20350

Dr. Bodo Kruger
Naval Electronics Systems Command Headquarters
Special Communications Project Office (PME-117)
National Center #1
Washington, DC 20360

Dr. Franklin Moore
Command and Control Technical Center
Room 133
11440 Issac Newton Square, No.
Reston, VA 22090

Professor Theodore R. Madden
Department of Earth and Planetary Sciences
Massachusetts Institute of Technology
Room 54-614
Cambridge, MA 02139

Professor George V. Keller
Colorado School of Mines
Department of Geophysics
Golden, CO 80401

Professor Stanley H. Ward
Department of Geological & Geophysical Sciences
University of Utah
Salt Lake City, UT 84112

Dr. James R. Wait, Senior Scientist
Environmnetal Research Laboratory
U.S. Department of Commerce
Room 242, Research Bldg. #1
Boulder, CO 80302

Dr. Bert Smith
Army Foreign Science & Technology Center
Department of the Army (DRXST-SD)
220 7th Street, N.E.
Charlottesville, VA 22901

Mr. D.D. Crombie, Associate Director
Office of Telecommunications
Institute for Telecommunication Sciences
U.S. Department of Commerce
Boulder, CO 80302

Professor Clarence S. Clay
Department of Geology and Geophysics
The University of Wisconsin
1215 W. Dayton Street
Madison, WI 53706

Mr. John Doncarlos, PME-117T
Naval Electronics Systems Command Headquarters
Special Communications Project Office
National Center #1
Washington, DC 20360

Dr. Arthur Dodd
Army Research Office
P.O. Box CM
Duke Station
Durham, NC 27706

Professor Jack Oliver
Chairman, Department of Geological Sciences
Cornell University
Ithaca, NY 14850

Mr. Edward Wolkoff
Naval Underwater Systems Center
New London Laboratory
New London, CT 06320

Professor Mark Landisman
Geosciences Division
University of Texas at Dallas
Richardson, TX 75080

Professor Frank Morrison
Engineering Geosciences
Hearst Mining Bldg.
Berkeley, CA 94720

Dr. Donal Miller
Code SA 3
Naval Underwater Systems Center
New London Laboratory
New London, CT 06320

Professor Gene Simmons
Department of Earth and Planetary Sciences
Massachusetts Institute of Technology
Bldg. 54-314
Cambridge, MA 02138

Mr. Richard G. Barakat
Bolt, Beranek and Newman, Inc.
50 Moulton Street
Cambridge, MA 02138

Dr. Steve Mock
Army Research Office
P.O. Box CM
Duke Station
Durham, NC 27706

Dr. Arthur F. Kuches
Cornell University
Department of Physics
Ithaca, NY 14850

Professor George C. Kennedy
University of California
Institute of Geophysics and Planetary Physics
Los Angeles, CA 90024

Professor Robert P. Meyer
Geophysical and Polar Research Center
Lewis G. Weeks Hall
1215 West Dayton Street
Madison, WI 53706

UNCLASSIFIED

SECURITY CLASSIFICATION OF THIS PAGE (When Data Entered)

REPORT DOCUMENTATION PAGE		READ INSTRUCTIONS BEFORE COMPLETING FORM
1. REPORT NUMBER Final Technical Report	2. GOVT ACCESSION NO.	3. RECIPIENT'S CATALOG NUMBER
4. TITLE (and Subtitle) MAGNETOTELLURIC AND DC DIPOLE-DIPOLE SOUNDINGS IN NORTHERN WISCONSIN		5. TYPE OF REPORT & PERIOD COVERED Final Technical 6. PERFORMING ORG. REPORT NUMBER
7. AUTHOR(s) F.X. Bostick, Jr., H.W. Smith, and J.E. Boehl		8. CONTRACT OR GRANT NUMBER(s) ONR Contract N00014-76-C-0484 and NSF Grant GA 38827
9. PERFORMING ORGANIZATION NAME AND ADDRESS Electrical Geophysics Research Laboratory ENS 623, The University of Texas at Austin, Austin, TX 78712		10. PROGRAM ELEMENT, PROJECT, TASK AREA & WORK UNIT NUMBERS
11. CONTROLLING OFFICE NAME AND ADDRESS Earth Physics Program, Code 463 Office of Naval Research Arlington, VA 22217		12. REPORT DATE May 15, 1977 13. NUMBER OF PAGES 52
14. MONITORING AGENCY NAME & ADDRESS(if different from Controlling Office)		15. SECURITY CLASS. (of this report) UNCLASSIFIED 15a. DECLASSIFICATION/DOWNGRADING SCHEDULE

16. DISTRIBUTION STATEMENT (of this Report)

Approved for public release; distribution unlimited.

17. DISTRIBUTION STATEMENT (of the abstract entered in Block 20, if different from Report)

18. SUPPLEMENTARY NOTES

19. KEY WORDS (Continue on reverse side if necessary and identify by block number)

MAGNETOTELLURICS
DC DIPOLE-DIPOLE
EARTH RESISTIVITY

20. ABSTRACT (Continue on reverse side if necessary and identify by block number)

During the summer of 1974 this Laboratory participated in a joint study of the crust in northern Wisconsin with the Colorado School of Mines, the University of Wisconsin at Madison and others. The Wisconsin Arch region was selected for the large areal extent of outcrop of highly resistive crystalline basement rocks considered most favorable for possible lithospheric propagation of low frequency electromagnetic waves. The principal objective of the joint

DD FORM 1 JAN 73 1473 EDITION OF 1 NOV 65 IS OBSOLETE

UNCLASSIFIED 410 133

SECURITY CLASSIFICATION OF THIS PAGE (When Data Entered)

study was the determination of the maximum resistivity and thickness of a highly resistant zone underlying a thin surface layer of glacial till over most of the area. It was recognized at the outset that a combination of deep DC resistivity sounding, which can determine the resistivity-thickness product of the resistant zone, and the magnetotelluric method, which can determine its thickness, would be required. DC dipole-dipole measurements made at 21 sites in the area encountered a highly conductive feature to the southeast of the fixed source dipole antennas in the direction of the maximum lateral extent of the outcrop. This feature, which is referred to as the Flambeau Anomaly, attenuated the transmissions from the dipole antennas and thus distorted the resistivity-thickness product results obtained by this Laboratory. However, magnetotelluric soundings provided estimates for the thickness of the resistant zone in the region southeast of the anomaly where DC dipole-dipole results by the Colorado School of Mines group indicate very high values for the resistivity-thickness products. By combining these results it is possible to estimate the resistivity of the resistant zone and its thickness. Results of this survey are presented along with some innovative methods for the analysis and inversion of magnetotelluric data.